




Late Cretaceous arc igneous activity: the Eđrikar Monzogranite example

F. Sipahi, A. Kaygusuz, Ç. Saydam Eker, A. Vural & İ. Akpınar


To cite this article: F. Sipahi, A. Kaygusuz, Ç. Saydam Eker, A. Vural & İ. Akpınar (2018) Late Cretaceous arc igneous activity: the Eđrikar Monzogranite example, International Geology Review, 60:3, 382-400, DOI: [10.1080/00206814.2017.1336120](https://doi.org/10.1080/00206814.2017.1336120)

To link to this article: <https://doi.org/10.1080/00206814.2017.1336120>

 View supplementary material 

 Published online: 08 Jun 2017.

 Submit your article to this journal 

 Article views: 106

 View related articles 

 View Crossmark data 



Late Cretaceous arc igneous activity: the Eğrikar Monzogranite example

F. Sipahi, A. Kaygusuz, Ç. Saydam Eker, A. Vural and İ. Akpınar

Department of Geology Engineering, Gümüşhane University, TR-2900, Gümüşhane, Turkey

ABSTRACT

The geochemical and Sr–Nd–Pb isotope properties, as well as the Laser Ablation Inductively Coupled Plasma and Mass Spectrometry (LA-ICP-MS) U–Pb zircon age, of Eğrikar Monzogranite in the eastern Pontides, are primarily investigated in this study with the aim of determining its magma source and geodynamic evolution. The U–Pb zircon age obtained from Eğrikar Monzogranite is 78 ± 1.5 Ma, thereby reflecting the age of monzogranite. The I-type Eğrikar Monzogranite comprises quartz, plagioclase (An_{35-45}), orthoclase, muscovite, and biotite. The geochemical analyses of the Eğrikar Monzogranite indicate being medium K calc-alkaline, peraluminous, and resembling magmatic arc granite. The Eğrikar Monzogranite is enriched in large ion lithophile elements and light rare earth elements relative to high field strength elements. Chondrite-normalized rare earth element patterns have concave upward shapes (La_N/Yb_N 2.47–8.58) with pronounced negative Eu anomalies ($Eu_N/Eu^* = 0.29-0.65$). Initial $\epsilon Nd_{(t)}$ values vary between 1.85 and 2.18 and initial $^{87}Sr/^{86}Sr$ values between 0.7048 and 0.7067. Fractionation of plagioclase, hornblende, and apatite played an important role in the evolution of Eğrikar Monzogranite. The crystallization temperatures of the melts ranged from 770°C to 919°C based on zircon and apatite saturation temperatures. The geochemical and isotopic data suggest being generated by the partial melting of mafic lower crustal sources.

ARTICLE HISTORY

Received 1 November 2016
Accepted 25 May 2017

KEYWORDS

Eğrikar Monzogranite;
LA-ICP-MS U–Pb zircon
dating; Late Cretaceous;
Sr–Nd–Pb isotopes; NE
Turkey

1. Introduction

Medium K calc-alkaline and I-type plutons, including subduction-related magmatic suites, have shown similarities in many convergent tectonic settings. Investigation and genetic classifications of plutonic rocks are based on the crustal, mantle, or mixed components; variable melting conditions; fractional crystallization (FC); and crustal contamination during their petrogenesis (Chappell and White 1992; Roberts and Clemens 1993; Thompson and Connolly 1995; Altherr and Siebel 2002; Chen *et al.* 2002). The Alpine–Himalayan orogenic belt in Turkey, which is between the Eurasia and Africa-Arabia plates, lies in an important geodynamic position. The structure of the southern coast of the Black Sea in the north of Turkey is an east–west trending and south-dipping reverse fault and Black Sea basin is known as a back arc basin during Cretaceous times (Nikishin *et al.* 2003). The Black Sea region (i.e. Turkey) represents a well-preserved continental magmatic arc (Dokuz *et al.* 2010; Eyüboğlu *et al.* 2011), which resulted from the subduction of the Neotethyan oceanic crust beneath the Eurasian plate during the Senonian epoch, and includes various intrusive and eruptive rocks (Figure 1(a)). Moreover, the Black Sea region is important for metallogenic provinces and includes many types of ore deposits

(e.g. volcanogenic massive sulphide, porphyry copper, skarn, and epithermal vein-types deposits). During the geological duration, granitoids are important for the evolution and development of the continental crust, as well as the formation of ore deposits (Sipahi 2011; Sipahi and Sadıklar 2011; Eyüboğlu *et al.* 2015; Akaryalı 2016; Akaryalı and Akbulut 2016). The ages of plutonic rocks in the eastern Black Sea region change from Paleozoic (Topuz *et al.* 2010; Kaygusuz *et al.* 2012a, 2016) to Cretaceous (Yılmaz *et al.* 2000; Boztuğ *et al.* 2006; Karslı *et al.* 2010; Kaygusuz and Aydınçakır 2011; Kaygusuz and Şen 2011; Sipahi 2011; Kaygusuz *et al.* 2013, 2014) and Eocene (Boztuğ *et al.* 2004; Topuz *et al.* 2005; Yılmaz-Şahin 2005; Eyüboğlu *et al.* 2011a; Figure 1(b); Table 1). The geochemical and isotopic characteristics of the Late Cretaceous granitoidic rocks in eastern Pontides were described by some researchers (Figure 2(a); Table 1). The emplacements of these plutons, from high-K calc-alkaline metaluminous–peraluminous to alkaline compositions, range from arc-collisional through syn-collisional to post-collisional (Yılmaz and Boztuğ 1996; Okay and Şahintürk 1997; Yılmaz *et al.* 1997; Boztuğ *et al.* 2003; Arslan and Aslan 2006).

In the Eğrikar area of the Gümüşhane from the eastern Black Sea region, arc-related magmatism developed

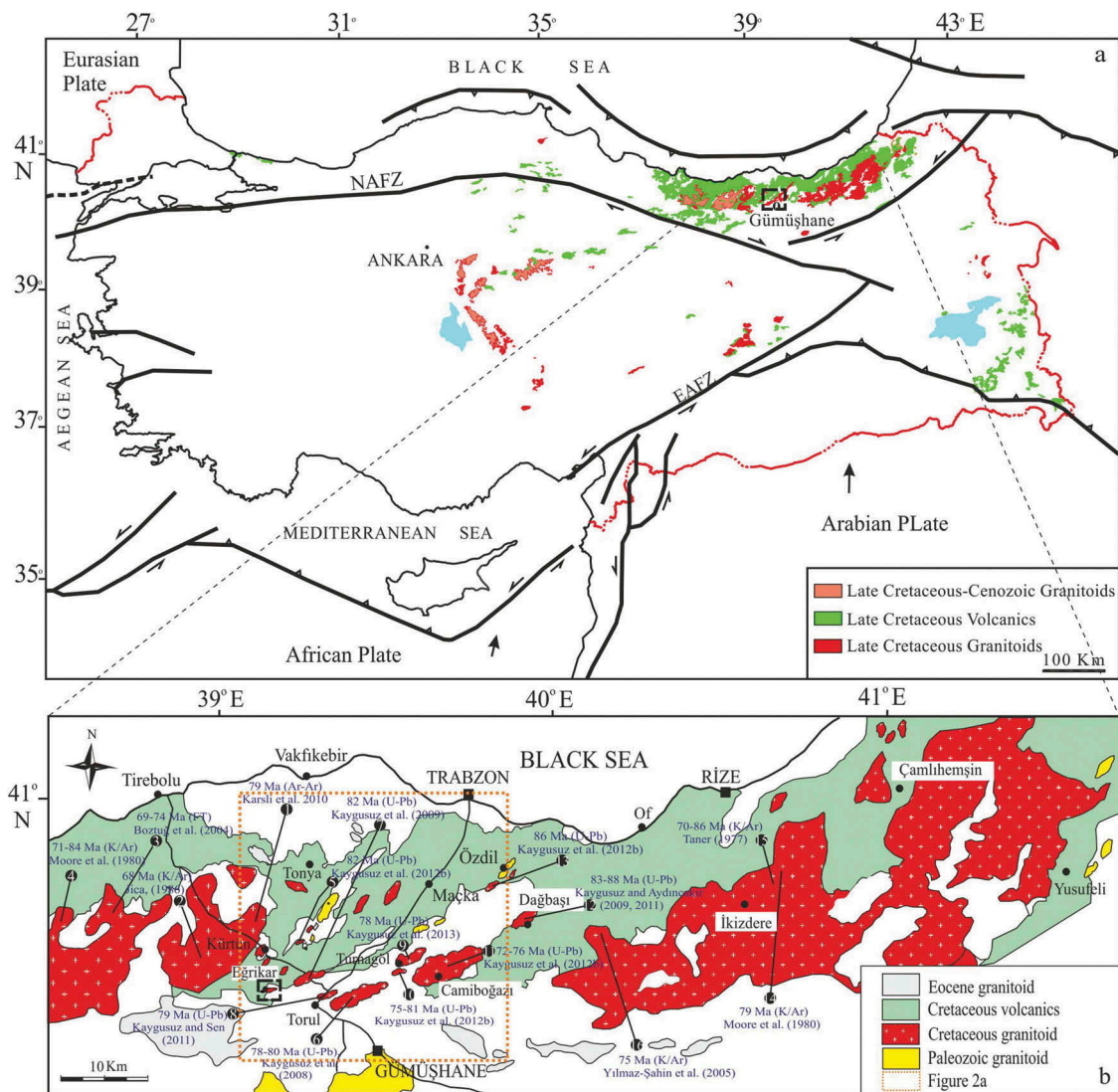


Figure 1. (a) Tectonic and Late Cretaceous magmatic rocks map of Turkey (modified after MTA 2011) and (b) simplified geological map showing the granitoid distribution in the Eastern Pontides (modified after Gedik *et al.* 1992). NAFZ: North-Anatolian fault zone; EAFZ: East-Anatolian fault zone; DSFZ: Dead Sea fault zone.

under a compressional regime and is characterized by the predominance of calc-alkaline monzogranite. Prior to the current research, knowledge on the geochronological age, as well as the geochemical and isotopic data, of Eğrikar Monzogranite was uncertain. The present study primarily discusses the detailed petrography, whole-rock geochemistry, Sr–Nd–Pb isotope compositions, and U–Pb zircon age of this monzogranite to determine its magma source and evolution.

2. Regional geology

The Black Sea region of Turkey are known as Pontides (Şengör and Yılmaz 1981; Okay and Tüysüz 1999). The Pontides belt extending between the Lesser Caucasus in the east and the Balkans in the west is divided into western

Pontides, Central Pontides, and eastern Pontides because of the different tectonic units. The eastern Pontides is distinguished from the western Pontides by the presence of a large volume of magmatic rocks (Okay and Şahintürk 1997; Okay and Tüysüz 1999). The investigated area is located in the eastern Pontides, which is a magmatic arc, block-faulted tectonic formation with subduction playing a role in the settlement of granitoids from the Permo–Carboniferous to the Eocene periods during the subduction of the Tethyan oceanic crust (Gedikoğlu 1978; Şengör and Yılmaz 1981). The basement of the eastern Black Sea region consists of early Carboniferous metamorphic rocks and Late Carboniferous granitoids (Topuz *et al.* 2010; Dokuz 2011; Kaygusuz *et al.* 2012a, 2016). Jurassic volcanic rocks found unconformably on the basement of the eastern Black Sea region. Jurassic volcano-sedimentary rocks

Table 1. The compilation of geochronological data of Late Cretaceous plutons from the eastern Pontides in NE Turkey.

Locations in Figure 2a	Rock type	Age (Ma)	Method	Reference
1-Harşit	q-Monzonite	79 ± 4.3	Ar–Ar	Karslı <i>et al.</i> (2010)
2-Kürtün	Granodiorite	68.4 ± 3.4	K/Ar	Jica (1986)
3-South of Dereli	Granodiorite	78.3 ± 1.5	K/Ar	Moore <i>et al.</i> (1980)
	Granodiorite	69.4 ± 2.7–74.1±2.9	Fission track (apatite)	Boztuğ <i>et al.</i> (2004)
4- East of Dereli	Granodiorite	71.4 ± 1.0–84.0±1.6	K/Ar	Moore <i>et al.</i> (1980)
5-Arpaçköy	Diorite	82.00 ± 2.3	U–Pb (zircon)	Kaygusuz <i>et al.</i> (2012b)
6-Torul	Syenogranite	77.9 ± 0.3	Rb/Sr	Kaygusuz <i>et al.</i> (2008)
	Biotite hornblende monzogranite	80.1 ± 1.6	U–Pb (zircon)	Kaygusuz <i>et al.</i> (2010)
	q-Monzodiorite	79.8 ± 1.2	U–Pb (zircon)	Kaygusuz <i>et al.</i> (2010)
	q-Monzonite	78.8 ± 1.2	U–Pb (zircon)	Kaygusuz <i>et al.</i> (2010)
7-Sariosman	hornblende monzogranite	82.7 ± 1.5	U–Pb (zircon)	Kaygusuz <i>et al.</i> (2009)
8-Köprübaşı	Granodiorite	79.3 ± 1.4	U–Pb (zircon)	Kaygusuz and Şen (2011); Kaygusuz <i>et al.</i> (2012b)
9-Turnagöl	Granodiorite	78.07 ± 0.73	U–Pb (zircon)	Kaygusuz <i>et al.</i> (2013)
10-Ayeser	q-Monzonite	74.73 ± 0.86	U–Pb (zircon)	Kaygusuz <i>et al.</i> (2012b)
11-Camiboğazı	q-Monzonite	72.48 ± 0.89	U–Pb (zircon)	Kaygusuz <i>et al.</i> (2014)
	Diorite	76.21 ± 0.79	U–Pb (zircon)	Kaygusuz <i>et al.</i> (2014)
	Monzogranite	75.04 ± 0.83	U–Pb (zircon)	Kaygusuz <i>et al.</i> (2014)
	Monzodiorite	75.65 ± 0.50	U–Pb (zircon)	Kaygusuz <i>et al.</i> (2014)
12-Dağbaşı	Tonalite	88.1 ± 1.7	U–Pb (zircon)	Kaygusuz and Aydınçakır (2009)
	Granodiorite	86.0 ± 2.0	U–Pb (zircon)	Kaygusuz and Aydınçakır (2009)
	Monzogranite	82.9 ± 1.3	U–Pb (zircon)	Kaygusuz and Aydınçakır (2009)
13-Oyman	Granite	86.82 ± 0.58	U–Pb (zircon)	Kaygusuz <i>et al.</i> (2012b)
14-İkizdere	Granodiorite	79.3 ± 1.0	K/Ar	Moore <i>et al.</i> (1980)
15-İkizdere	Granodiorite	70.6 ± 0.5–80.7±0.6	K/Ar	Taner (1977)
16-Araklı	Granodiorite	75.7 ± 1.55	K/Ar	Yılmaz-Şahin (2005)

developed in an extension setting being possibly related to rifting (Arslan *et al.* 1997; Şen 2007; Saydam Eker *et al.* 2012). These rocks are overlaid conformably by the Middle–Late Jurassic and Cretaceous carbonates (Okay and Şahintürk 1997). The Late Cretaceous units unconformably overlying these carbonate rocks consist of sedimentary rocks in the southern part and volcanic rocks in the northern part of the eastern Black Sea region (Yılmaz and Korkmaz 1999). Late Cretaceous volcanic rocks are mainly tholeiitic and calc-alkaline and display typical island arc characteristics (Çamur *et al.* 1996; Arslan *et al.* 1997; Sipahi and Sadıklar 2014; Sipahi *et al.* 2014). The Late Cretaceous aged calc-alkaline volcanic arc-related series were likely formed during closure of the Neo-Tethys Ocean (Rolland *et al.* 2010). Several granitoidic rocks were emplaced into the magmatic arc that was active during the Jurassic and Paleocene times. Plutonic rocks, such as Dağbaşı Pluton (Kaygusuz and Aydınçakır 2011), Harşit pluton (Karslı *et al.* 2010), Torul pluton (Kaygusuz *et al.* 2010), Köprübaşı Pluton (Kaygusuz and Şen 2011), Turnagöl Plutons (Kaygusuz *et al.* 2013), and Camiboğazı Pluton (Kaygusuz *et al.* 2014), have been regarded as products of north-vergent subduction of Neotethyan oceanic crust. In addition, Early Cretaceous subduction-related calc-alkaline magmatism is a good indicator for porphyry Cu–Mo systems in the eastern part of the eastern Pontides (Delibaş *et al.* 2016). Eocene volcanic and sedimentary rocks unconformably overlie the Late Cretaceous series (Aydınçakır 2014; Aydınçakır and Şen

2014; Yücel *et al.* 2014). The eastern Black Sea region remained above sea level probably because of the collision between the magmatic arc and the Tauride–Anatolide block from the Paleocene to early Eocene (Okay and Şahintürk 1997; Boztuğ *et al.* 2004).

3. Analytical methods

3.1. Whole-rock geochemical analyses

A total of 20 samples were obtained from Eğrikar Granitoid. The modal mineralogy of these samples was determined through point counting using a Swift automatic counter fitted to a polarizing microscope in Gümüşhane University, Department of Geology Engineering (Supplementary Table 1). Microscopic studies resulted in 12 representative samples being selected for major, trace, and rare earth element (REE) analyses that were performed at the commercial ACME Laboratories, Ltd. (Vancouver, Canada). Major elements were measured by inductively coupled plasma–atomic emission spectrometry after fusion with LiBO₂. The 0.2 g of sample powder and 1.5 g of LiBO₂ flux were mixed in a graphite crucible and subsequently heated to 1050°C for 15 min for trace elements and REE analyses. Detection limits are in the range of 0.01–0.1 wt% for the major oxides, 0.1–10 ppm for the trace elements, and 0.01–0.5 ppm for REEs.

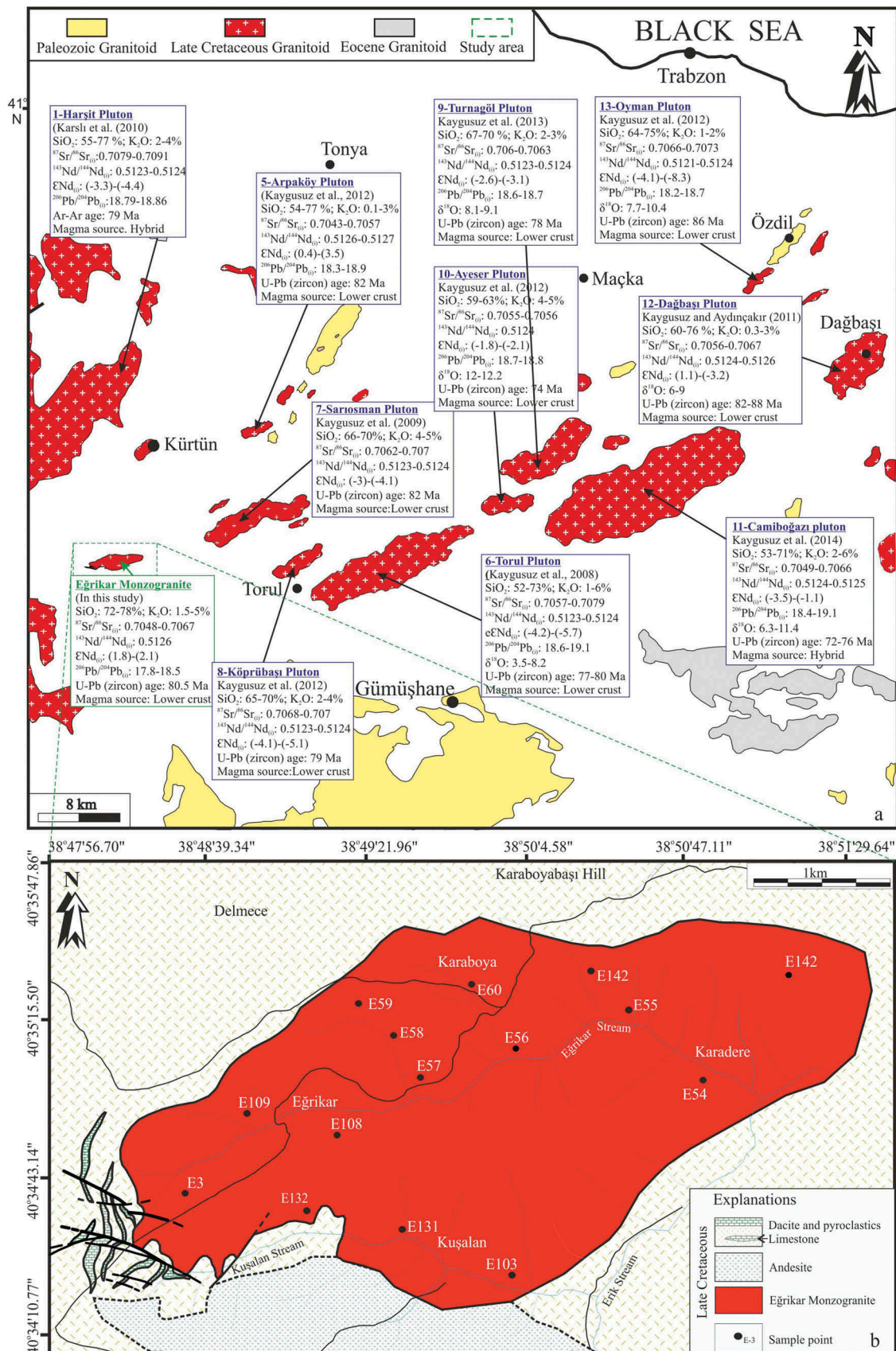


Figure 2. (a) The age, some geochemical and isotopic characteristics of the Late Cretaceous plutonic rocks and (b) Simplified geological map of the study area.

3.2. Sr, Nd, and Pb isotopes analyses

Sr, Nd, and Pb isotopic analyses were conducted at the Department of Geological Sciences, New Mexico State University. Isotopic measurements were made by TIMS on a VG Sector 30 mass spectrometer. Samples analysed were loaded onto rhenium filaments on either Cathodian beads of single filament only or on the side filament of a triple filament assembly. Reproducibility of the $^{87}\text{Rb}/^{86}\text{Sr}$ and $^{147}\text{Sm}/^{144}\text{Nd}$ ratios are within 0.3%, and the $^{87}\text{Sr}/^{86}\text{Sr}$ and $^{143}\text{Nd}/^{144}\text{Nd}$ ratios are within ± 0.000025 and ± 0.00003 , respectively. An analysis of the NBS 987 standard yielded values of 0.710226 (11), 0.710213 (13), 0.710219 (10), and 0.710260 (11). Pb samples were analysed using the middle filament position of a Cathodian bead assembly. Samples were loaded using 5% HNO_3 and in a matrix of silica gel and phosphoric acid. Approximately 2 μL of silica gel was positioned on the filament and 1 μL of phosphoric acid was added. Standards were also loaded and analysed using the same procedures. The mean of standard runs was $^{206}\text{Pb}/^{204}\text{Pb} = 16.844$, $^{207}\text{Pb}/^{204}\text{Pb} = 15.379$, and $^{208}\text{Pb}/^{204}\text{Pb} = 36.199$. Deviations of the standards are within 0.2%. Ramos (1992) provided the detailed analytical procedures for the Sr and Nd isotopic measurements.

3.3. U–Pb zircon dating analysis

U–Pb zircon dating was performed using LA–ICP–MS at the Geologic Laboratory Center, China University of Geosciences (Beijing, China). Zircon grains for U–Pb dating were extracted using heavy-liquid and magnetic separation methods and further purified by hand picking under a binocular microscope. Selected grains were mounted on an epoxy resin and polished half-way through. Cathodoluminescence images were used to examine the internal structures of individual zircon grains and to ensure an effective selection of analytical positions. A quadrupole ICP–MS apparatus (Agilent 7500a) was connected to a UP-193 solid-state laser (193 nm, New Wave Research Inc.) with an automatic positioning system. Laser spot size, energy density, and repetition rate were set to approximately 36 μm , 8.5 J/ cm^2 , and 10 Hz, respectively. The ablated material was transported into ICP–MS by a high-purity He gas stream with a flux of 0.8 L/min. The U–Pb isotopic fractionation effects were corrected using zircon 91500 (Wiedenbeck *et al.* 1995) as an external standard. Zircon standard TEMORA (417 Ma, Black *et al.* 2003) was also used as a secondary standard to monitor the deviation of age measurement/calculation. A total of 10 analyses of TEMORA yielded the apparent $^{206}\text{Pb}/^{238}\text{U}$ ages of 417–

418 Ma. The isotopic ratios and elemental concentrations of zircon were calculated using GLITTER software (ver. 4.4, Macquarie University). Uncertainties on age data are given as 1 sigma level. Concordia ages and diagrams were made using Isoplot/Ex (3.0) (Ludwig 2003). Common lead was corrected following the method of Andersen (2002).

4. Results

4.1. Petrography

Eğrikar Monzogranite is located approximately 100 km northwest of Gümüşhane, exhibits an NE–SW elongated shape, and covers an area of approximately 11 km^2 (Figure 2(b)). The shape of the monzogranite is elliptical, although it is slightly deformed and altered. The country rocks around Eğrikar Monzogranite comprise Late Cretaceous volcanic and sedimentary rocks (Figure 2(b)). Late Cretaceous volcanic rocks consist of andesite and dacite and their pyroclastics from lowermost to uppermost, respectively. Volcanic rocks include limestone (the middle-upper Maastrichtian age based on paleontological (*Rosita contusa* (Cushman), *Gansserina gansseri* (Bolli), *Globotruncana cf. bulloides* Vogler, *Globotruncanita cf. conica* (White), and *Globotruncana ventricosa* (White)) evidence) in the study area (Figure 2(b)). It is not seen any mineralization in the contact between volcanic and monzogranite. No enclaves are observed in the Eğrikar Monzogranite. The Eğrikar Monzogranite is pink to pinkish grey with medium granular; myrmekitic, and graphic textures comprise quartz (33%–46%), plagioclase (26%–34%), orthoclase (16%–21%), muscovite (1%–6%), biotite (1%–5%), and magnetite and pyrite as opaque minerals (Supplementary Table 1; Figure 3). Zircon occurs as an accessory mineral. Epidote, sericite, and chlorite are secondary phases. The Eğrikar Monzogranite generally shows physical alteration towards the east side. The rocks of the Eğrikar Monzogranite fall into the field of monzogranite in the QAP (quartz–alkali feldspar–plagioclase) modal mineralogical classification diagram (Streckeisen 1976) and are compared other Late Cretaceous granitoidic rocks in the eastern Pontides from NE Turkey (Figure 4). In the Eğrikar Monzogranite, quartz is anhedral with irregular cracks, is interstitial between other minerals, and generally shows undulose extinction. Quartz size becomes increasingly smaller in the contact zones between the country rocks. Plagioclase forms mostly subhedral to anhedral prismatic and lath-shaped crystals. The grain sizes of plagioclase vary from 0.3 to 1 mm for large crystals. Plagioclase shows albite twinning and

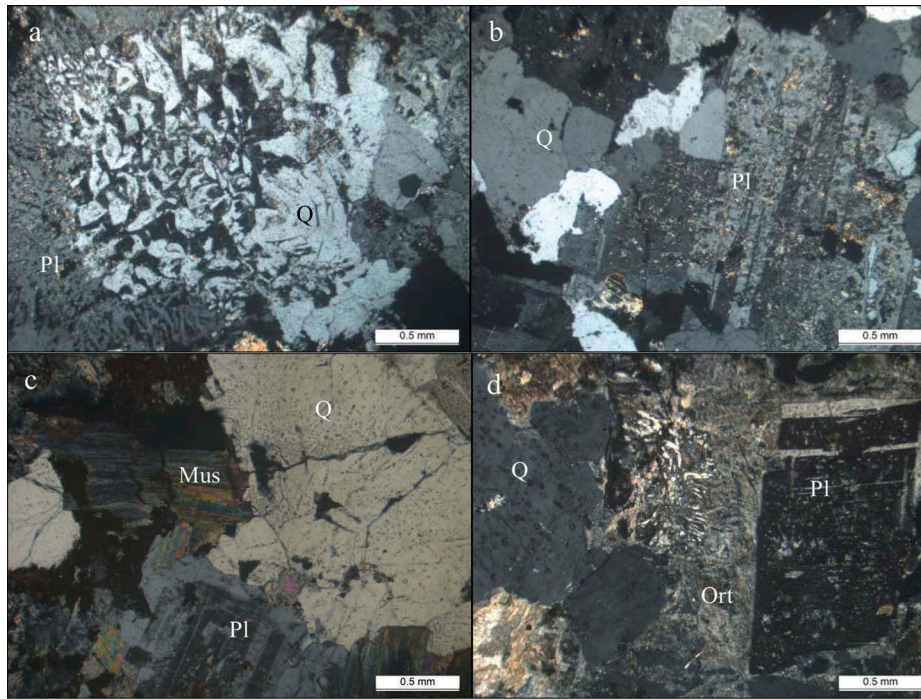


Figure 3. The textures of the Eğrikar Monzogranite. (a) Graphic texture (Samp. No.: E-108), (b) and (c) Granular texture (Samp. No.: E-109 and E-59) and (d) Myrmekitic granular texture (Sample No.: E-103), Pl: Plagioclase, Q: Quartz, Ort: Orthoclase, Mus: Muscovite.

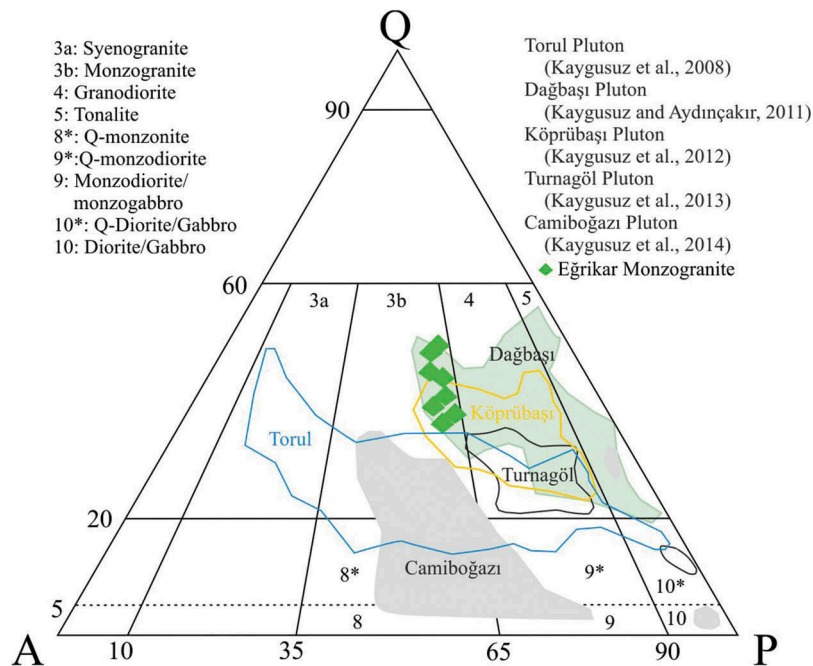


Figure 4. Modal mineralogical classification diagram (Streckeisen 1976). A: Alkali feldspar, P: Plagioclase, Q: Quartz.

andesine (An_{35-45}) compositions. Large plagioclase crystals may be altered to sericite and clay minerals. K-feldspars form anhedral to subhedral crystals. A myrmekitic texture is observed at the grain boundaries between quartz and orthoclase (Figure 3(d)). Alteration to clay minerals is common in the large K-feldspar

crystals. Biotite is subhedral and forms prismatic crystals. Biotite is reddish-brown and altered partially chloritized. Muscovite is a flake form and not the first-order aluminium silicate phase (Figure 3(c)). Euhedral zircon is an accessory phase in all rocks and forms short prismatic crystals. The petrographic compositions of the

Eğrikar Monzogranite have the difference from the other Late Cretaceous Turnagöl, Camiboğazi, Köprübaşı, Torul, Dağbaşı and Harşit plutonic rocks from the eastern Pontides in point of mafic mineral types, and not include hornblende and pyroxene minerals (Supplementary Table 1).

4.2. U–Pb zircon dating

Supplementary Table 2 presents the LA–ICP–MS U–Pb zircon dating results of Eğrikar Monzogranite. The U–Pb zircon dating results of Eğrikar Monzogranite as Concordia diagrams are shown in Figure 5. The Eğrikar Monzogranite sample E56 contains abundant zircon grains that are colourless, short to long prismatic, and euhedral (Figure 5(a)). The zircon grains are mostly fine-grained (i.e. 50–100 µm) and have aspect ratios of approximately 2. These grains show oscillatory zoning (Figure 5(a)). All of these features indicate that zircons are of magmatic origin (Pupin 1980). Most analyses yielded concordant age data. The $^{206}\text{Pb}/^{238}\text{U}$ age is 78 ± 1.5 Ma (MSWD % 0.95) (Supplementary Table 2; Figure 5(b)). For the Eğrikar Monzogranite, a Late Cretaceous age is established using the U–Pb zircon dating, and is interpreted as the magmatic emplacement age.

4.3. Geochemistry

Supplementary Table 3 shows the results of the geochemical analyses of the representative samples from Eğrikar Monzogranite. All samples fall in the granite field on the classification diagram of Middlemost (1994) (Figure 6(a)). Eğrikar Monzogranite has a narrow compositional range with SiO_2 and Al_2O_3 contents of approximately 72–78 wt% and 12–13 wt%, respectively (Supplementary Table 3). The Late Cretaceous granitoidic rocks in eastern Pontides have a compositional variation from diorite to granite. The majority of Late Cretaceous granitoidic rocks in the eastern Pontide belong to the medium to high-K calc-alkaline series (Figure 6(b,c)). The Eğrikar monzogranite is classified as medium-K calc-alkaline (approximately 1.5–2.3 wt% K_2O) as Torul, Turnagöl, Köprübaşı, Camiboğazi, and Dağbaşı plutons and peraluminous (aluminium saturation index = A/CNK [molecular $\text{Al}_2\text{O}_3/(\text{CaO}+\text{K}_2\text{O}+\text{Na}_2\text{O})$] values is from 1.04 to 2.12).

Harker plots of the selected major and trace elements from Eğrikar Monzogranite (Figure 7) show the linear variations in the element concentrations. The Al_2O_3 , CaO, MgO, $\text{Fe}_2\text{O}_{3\text{T}}$, TiO_2 , and P_2O_5 abundances decrease with increasing SiO_2 similar to the Harşit Pluton. Ba defines a positive correlation with increasing SiO_2 content (Figure 7). The Eğrikar Monzogranite and

Dağbaşı Pluton are depleted in Y compared to the other Late Cretaceous granitoidic rocks (Figure 7).

The general trend of the normal-MORB-normalized (Sun and McDonough 1989) element concentration diagram shows the enrichment of large-ion lithophile elements (LILEs) and the depletion of high-field-strength elements (HFSEs) of all samples (Figure 8(a)). The depletion in HFSEs is best expressed by the negative Nb, P, and Ti anomalies. The general trends of the normal-MORB-normalized element concentration of Eğrikar Monzogranite are similar to Dağbaşı, Harşit, and Jindong plutons; however, that of Camiboğazi, Turnagöl, and Köprübaşı plutons are slightly different on Sr (see Figure 8(a)). The samples of the Turnagöl and Camiboğazi plutons show the enrichment in LILEs and depletion in HFSEs, whereas Torul and Köprübaşı plutons display the enrichment in LILEs and HFSEs according to Eğrikar Monzogranite. The chondrite-normalized (Boynton 1984) REE patterns of the Eğrikar Monzogranite samples (Figure 8(b)) are characterized by concave-upward shapes ($\text{La}_\text{N}/\text{Yb}_\text{N}$ 2.47–8.58) and have negative Eu anomalies ($\text{Eu}_\text{N}/\text{Eu}^*$) of 0.29–0.65. The REE pattern of Eğrikar Monzogranite is similar to that of the Dağbaşı, Turnagöl, Camiboğazi, and Jindong plutons (see Figure 8(b)). The samples of the Köprübaşı, Turnagöl, and Camiboğazi plutons show the enrichment in LREEs and depletion in HREEs, whereas Torul and Köprübaşı plutons display the enrichment in LREEs and HREEs according to Eğrikar Monzogranite.

The tectonic setting of Eğrikar Monzogranite is interpreted by using various tectono-magmatic discrimination diagrams. The samples plot within the volcanic arc granite fields, as shown in the Nb vs. Y and Rb vs. (Y+Nb) diagrams (Pearce *et al.* 1984; Figure 9(a, b)), as well as the Rb/30–Hf–Tax3 ternary diagram (Harris *et al.* 1986; Figure 9(c)), and are similar to the Dağbaşı and Jindong plutons. In the (La/Yb) vs. (Th/Yb) diagram (Figure 9(d)), the Eğrikar Monzogranite, Dağbaşı, and Jindong plutons samples fall within the island arc and all samples can be classified as volcanic-arc granites, thereby setting emplacement in magmatic arc-related environment as supported from their LREE–LILE-enriched and depleted HFSE characteristics. In the tectonic discrimination diagram of Whalen *et al.* (1987), the Eğrikar Monzogranite and Dağbaşı Pluton samples fall within the I-type granite field (Figure 9(e)).

4.4. Zircon and apatite saturation temperature

Zircon and apatite saturation temperatures (Watson and Harrison 1983; Hanchar and Watson 2003; Miller

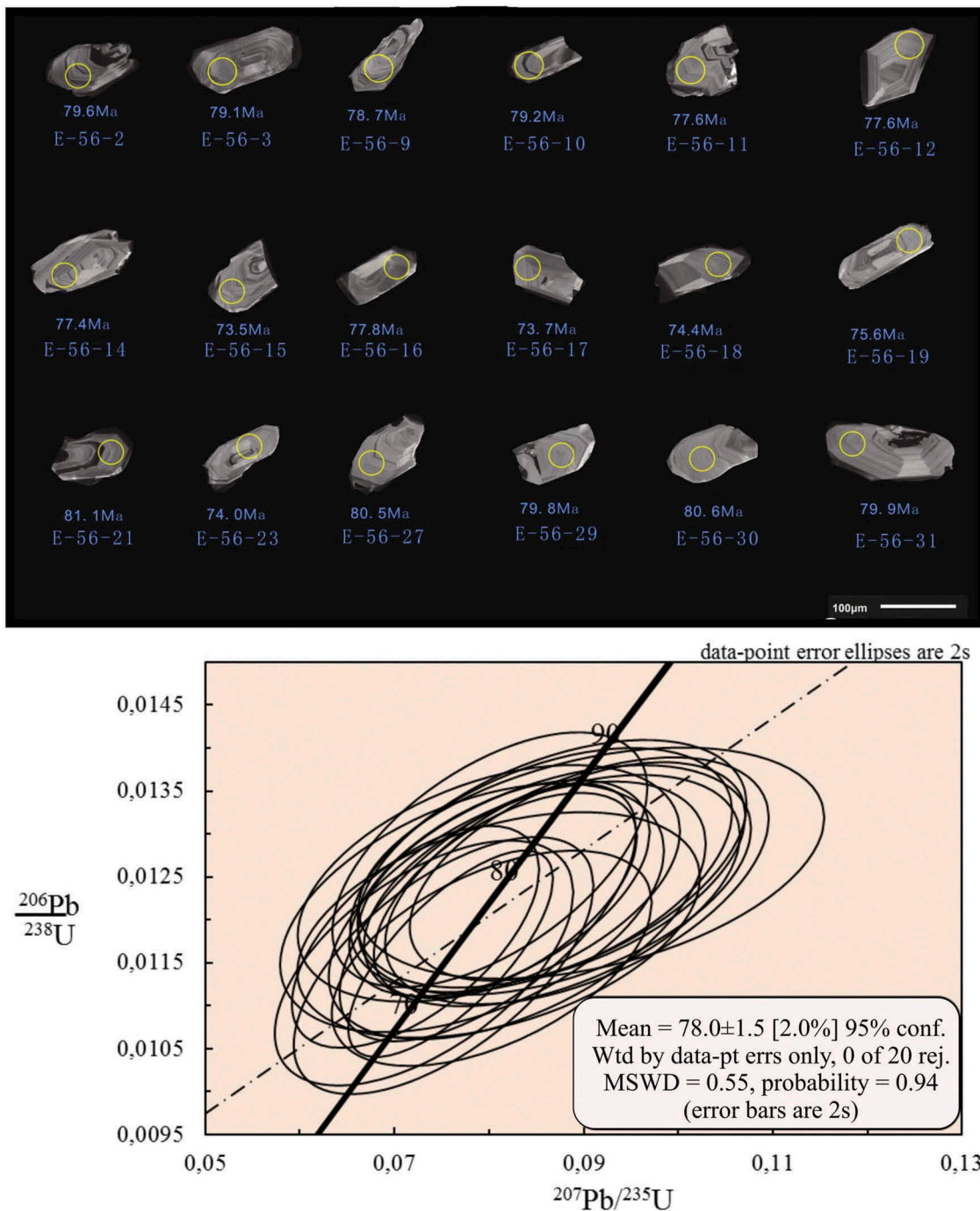


Figure 5. (a) CL images of zircons and (b) Concordia diagram showing LA-ICP-MS U-Pb analyses of zircons for sample E-56 from Eğrikar Monzogranite.

et al. 2003) in Eğrikar Monzogranite were calculated from the whole-rock geochemical data (see Supplementary Table 4). The Zr (65.1–161 ppm) and P_2O_5 (0.01–0.07 wt%) abundances in the Eğrikar Monzogranite samples result in zircon and apatite saturation temperatures. The calculated zircon saturation temperatures for Eğrikar Monzogranite range from 770°C to 819°C, whereas the apatite saturation temperature is between 793°C and 919°C. Subhedral zircon

grains appear in the rims of the quartz, orthoclase, and plagioclase grains. Thus, the crystallization of zircon started relatively late at temperatures lower than that of the intruding magma. This result is supported by the Zr abundances that are not systematically related to the SiO_2 concentration. Therefore, the calculated zircon saturation temperatures should be considerably lower than the temperature of the intruding magma (Figure 7 (e)). By contrast, apatite crystallization is thought to

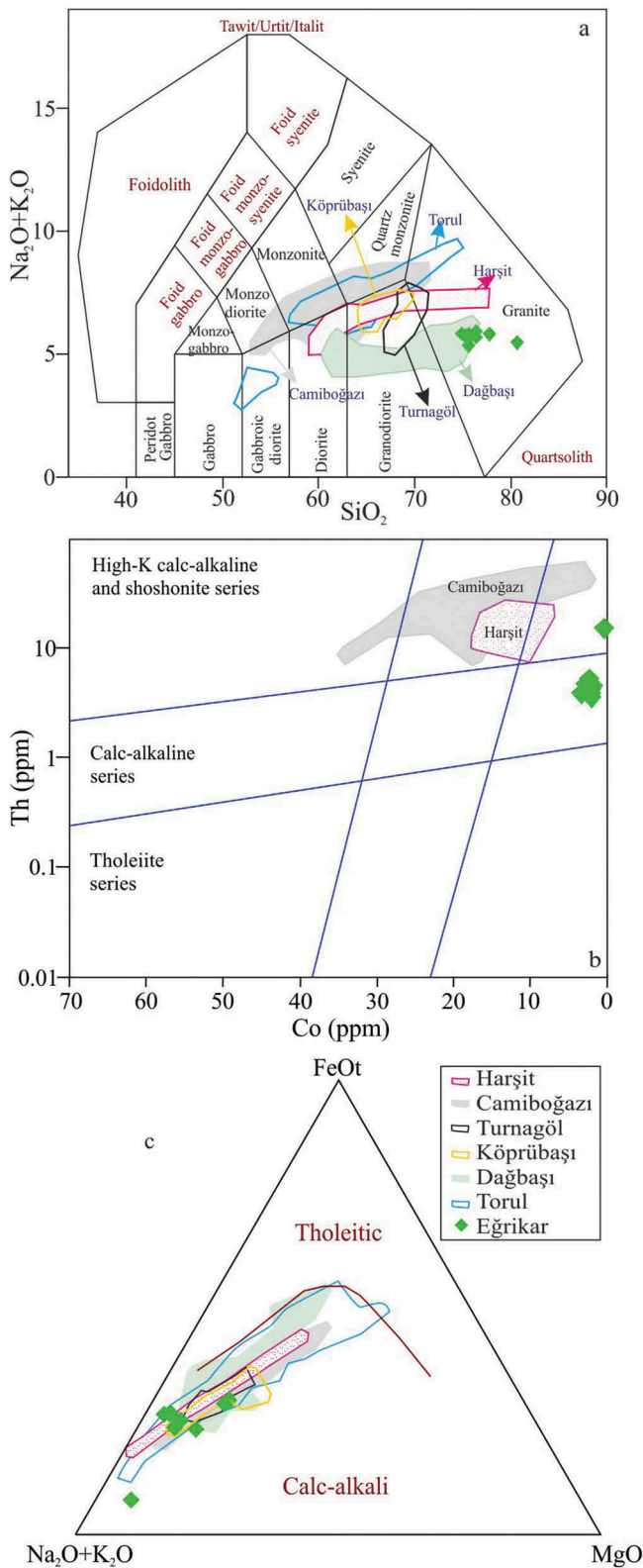


Figure 6. Chemical classification diagram (Middlemost 1994), (b) Co vs. Th discrimination diagram (Hastie *et al.* 2007) and (c) AFM diagram (Irvine and Baragar 1971) for samples from the Egridir Monzogranite.

have started considerably early because the apatite grains occur in early crystallized plagioclase, and the bulk-rock P_2O_5 content generally decreases with increasing SiO_2 (Figure 7(f)). Thus, the temperatures of the intruding magmas were probably not substantially higher than the calculated apatite saturation temperatures of 793–919°C.

4.5. Sr, Nd, and Pb isotopes

Supplementary Tables 6 and 7 list the Sr, Nd, and Pb isotopic data of the Egridir Monzogranite samples. The initial Sr, Nd, and Pb isotope ratios were calculated using the Rb, Sr, Sm, Nd, U, Th, and Pb concentration data obtained from the ICP–MS analyses by assuming a monzogranite age of 78 Ma. The Egridir Monzogranite samples exhibit a narrow range of initial $^{87}\text{Sr}/^{86}\text{Sr}$ ratios (0.7048–0.7064) and $\epsilon_{\text{Nd}(i)}$ values (1.85–2.18). The corresponding Nd model ages (T_{DM}) of the monzogranites range from 0.67 to 0.83 Ga. In the SiO_2 vs. $(^{87}\text{Sr}/^{86}\text{Sr})_i$ diagram, the $(^{87}\text{Sr}/^{86}\text{Sr})_i$ decreases with increase in SiO_2 (Figure 10(a)). In the SiO_2 vs. $(^{143}\text{Nd}/^{144}\text{Nd})_i$ diagram (Figure 10(b)), the samples define nearly horizontal trends that indicate FC. When Egridir Monzogranite is compared with other Cretaceous plutons from the eastern Black Sea region, the studied samples have $\epsilon_{\text{Nd}(i)}$ and $(^{87}\text{Sr}/^{86}\text{Sr})_i$ ratios similar to those of the Dağbaşı, Sarosman, and Turnagöl plutons but have slightly different $(^{87}\text{Sr}/^{86}\text{Sr})_i$ ratios than those from the Torul, Köprübaşı, and Harşit plutons (Figure 11). The Dağbaşı, Torul, Sarosman, Köprübaşı, and Harşit samples show a negative correlation between $\epsilon_{\text{Nd}(i)}$ and $(^{87}\text{Sr}/^{86}\text{Sr})_i$. By contrast, the Egridir Monzogranite and Turnagöl pluton samples show no evident correlation between these two parameters.

The Egridir Monzogranite samples have similar isotopic compositions: $(^{206}\text{Pb}/^{204}\text{Pb})_i = 17.86\text{--}18.58$, $(^{207}\text{Pb}/^{204}\text{Pb})_i = 15.57\text{--}15.64$, and $(^{208}\text{Pb}/^{204}\text{Pb})_i = 37.94\text{--}38.66$ (Supplementary Table 6; Figure 12). The Egridir Monzogranite samples fall within the fields of the lower continental crust (LCC) described by Kempton *et al.* (1997) and close to similar field of Turnagöl, Torul, Camiboğazı, and Jindong plutons (see Figure 12(a)). In the $(^{206}\text{Pb}/^{204}\text{Pb})_i$ vs. $(^{207}\text{Pb}/^{204}\text{Pb})_i$ and $(^{208}\text{Pb}/^{204}\text{Pb})_i$ diagrams (Figure 12), the studied samples were nearly found together with Torul, Turnagöl, and Camiboğazı plutons (Kaygusuz *et al.* 2008, 2013, 2014) and Jindong Pluton (Oh *et al.* 2016) which are in the field of arc magmas (Zartman and Doe 1981).

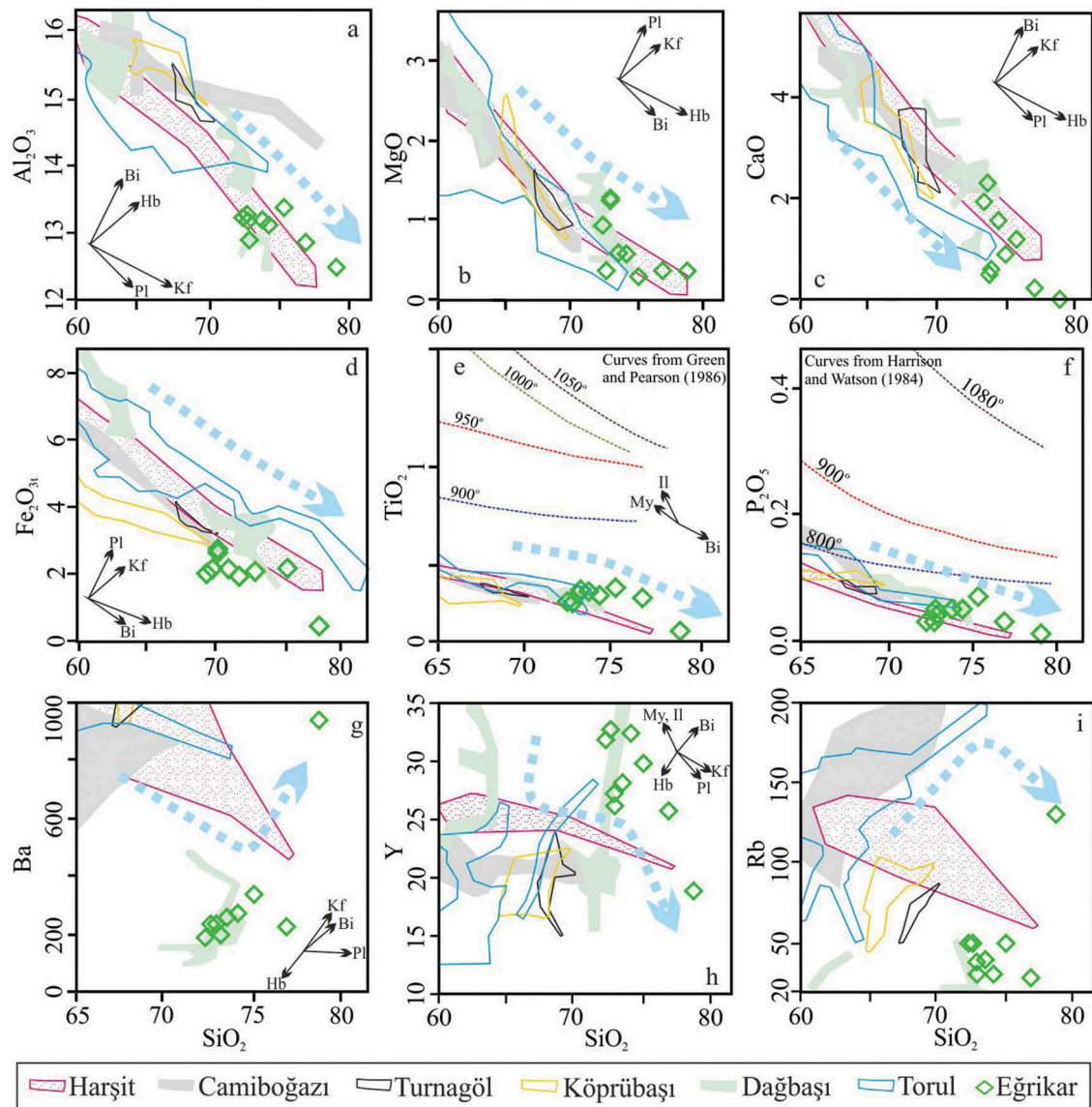


Figure 7. Variation diagrams of SiO_2 vs. major oxides (wt%) and trace elements (ppm) for samples from the Eğrikar Monzogranite. Blue arrows show fractional crystallization processes of minerals. Pl: Plagioclase, Kf: K-feldspar, Bi: Biotite, Hb: Hornblende, My: Magnetite, Il: Ilmenite.

5. Discussion

5.1. Age

The emplacement age of Eğrikar Monzogranite was estimated from stratigraphic criteria and contact relationships in a previous study. Such data are often imprecise because of rock deformation and tectonic setting. Information on the emplacement age of Eğrikar Monzogranite was not satisfactory for its geological setting. Unpublished General Directorate of Mineral Research and Exploration (MTA) reports conjectured that the age of the Eğrikar Monzogranite was Tertiary based on contact and stratigraphic criteria. Our new LA-ICP-MS U-Pb zircon age of Eğrikar Monzogranite is 78 ± 1.5 Ma

(Supplementary Table 5, Figure 5). This age is similar to the emplacement age of the Turnagöl Pluton (78.07 ± 0.73 Ma; Kaygusuz *et al.* 2013), monzogranite from Camiboğazı pluton (75.04 ± 0.3 Ma; Kaygusuz *et al.* 2014), monzogranite from Torul pluton (78.8 ± 1.2 Ma to 80.1 ± 1.6 Ma; Kaygusuz *et al.* 2010), granodiorite from Köprübaşı Pluton (79.3 ± 1.4 Ma; Kaygusuz and Şen 2011), monzogranite from Dağbaşı pluton (82.9 ± 1.3 Ma; Kaygusuz and Aydınçakır 2011), and monzogranite from Sarosman pluton (82.7 ± 1.5 Ma; Kaygusuz *et al.* 2009) (Table 1). A major pulse of Late Cretaceous igneous activity occurred around ~ 78 Ma from the existing data (Table 1) and the age of the Eğrikar Monzogranite in this study (78 Ma) coincides with this peak.

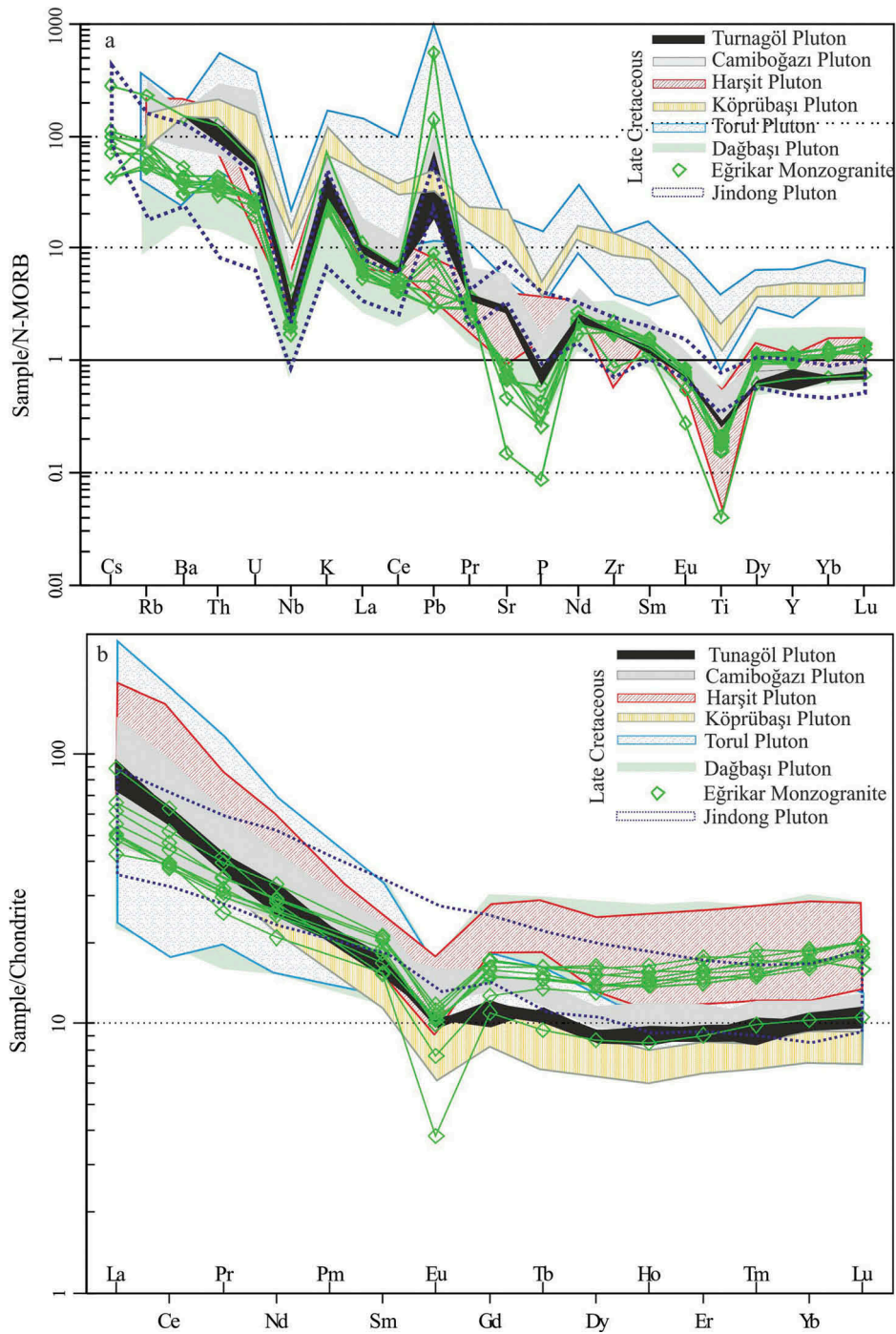


Figure 8. (a) The normalized N-MORB (Sun and McDonough 1989) and (b) Chondrite-normalized diagram (Boynton 1984) for samples from the Eğrikar Monzogranite.

5.2. Petrogenesis

Two main models have been proposed to interpret the petrogenesis and origin of the calc-alkaline intrusions such as the Eğrikar Monzogranite: (1) partial melting of the mafic lower crust at relatively high pressures (e.g. Roberts and Clemens 1993) or (2) derived from basaltic parent magmas by the FC or assimilation and FC

processes (e.g. Grove and Donnelly-Nolan 1986; Bacon and Drittt 1988). The Eğrikar Monzogranite samples are characterized by weak REE fractionation (La_N/Yb_N 2.47–8.58), negative Eu anomalies ($Eu_N/Eu^* = 0.29–0.65$), low Sr/Y ratios (0.70–3.18), high Y (18–32 ppm), and Yb (2.16–3.94 ppm) contents (Supplementary Table 3), negative Nb and Ta anomalies, and enrichment in

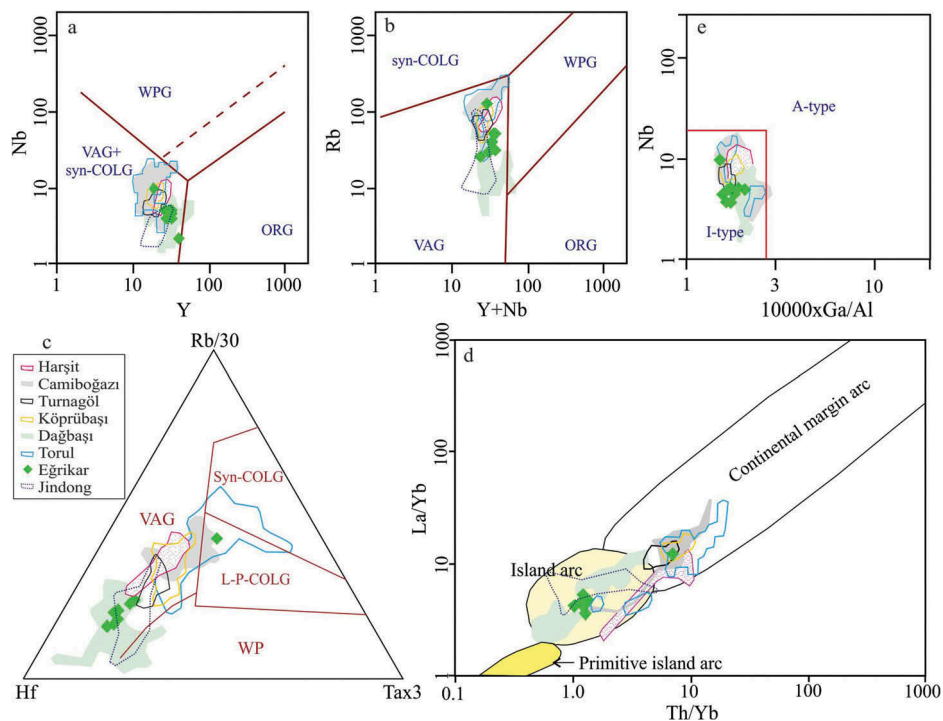


Figure 9. (a) Y vs. Nb diagram (Pearce *et al.* 1984), (b) Y+Nb vs. Rb diagram (Pearce *et al.* 1984), (c) Rb/30–Hf–Tax3 ternary diagram (Harris *et al.* 1986), (d) Th/Yb vs. La/Yb diagram and (e) (1000xGa/Al) vs. Nb classification diagram (Whalen *et al.* 1987) plot for samples from the Eğrikar Monzogranite. VAG: Volcanic-arc granites; Syn-COLG: Syncollisional granites; L-P-COLG: Late-post collisional granites; WPG: Within-plate granites; ORG: Ocean-ridge granites.

LILEs and LREEs. The Y content of Eğrikar Monzogranite has same with the Late Cretaceous Jindong Plutons (14–29 ppm; Oh *et al.* 2016) whereas the Sr (41–81 ppm) content of the Eğrikar Monzogranite ranges higher than the Jindong Plutons (307–687 ppm; Oh *et al.* 2016). A high Sr content is the FC of minerals that preferentially partition Y, such as amphibole, in the absence of the significant fractionation of plagioclase which prefers Sr (Kolb *et al.* 2013; Oh *et al.* 2016). The negative anomalies in Nb, P, and Ti reflect the characteristic of subduction-related magmas, which are often thought as the relative enrichment of the mantle source by the influx of LILE through slab dehydration (e.g. McCulloch and Gamble 1991). The negative anomalies in Nb, P, and Ti are formed by amphibole-dominated FC of the hydrous arc magma (Oh *et al.* 2016). The Eğrikar Monzogranite samples display relatively homogeneous isotopic compositions of $^{87}\text{Sr}/^{86}\text{Sr}_{(i)}$ ranging from 0.7048 to 0.7064, and of $\epsilon\text{Nd}_{(i)}$ from 1.85 to 2.18 (Supplementary Table 5). The corresponding Nd model ages (TDM) of the Eğrikar Monzogranite samples like Jindong Pluton, $\epsilon\text{Nd}_{(i)}$ was unchanged when the $^{87}\text{Sr}/^{86}\text{Sr}_{(i)}$ values were increased (Figure 11). The Eğrikar Monzogranite samples are relatively homogenous in isotopic compositions with $^{143}\text{Nd}/^{144}\text{Nd}_{(i)}$

ranging from 0.512658 to 0.512681, and $\epsilon\text{Nd}_{(i)}$ from 1.85 to 2.18. A narrow range in the $^{87}\text{Sr}/^{86}\text{Sr}_{(i)}$ ratios and $\epsilon\text{Nd}_{(i)}$ values of Eğrikar Monzogranite determine a depleted mantle source region enriched by slab components. The positive $\epsilon\text{Nd}_{(i)}$ values suggest a depleted mantle or mantle-derived end-member (Faure and Mensing 2005). The $^{87}\text{Sr}/^{86}\text{Sr}_{(i)}$ ratio of Eğrikar Monzogranite is similar to those of the dağbaşı (0.70561–0.70666), Camiboğazı (0.7049–0.7061), and Turnagöl (0.70601–0.70626) plutons. However, the $^{143}\text{Nd}/^{144}\text{Nd}_{(i)}$ ratios of Eğrikar Monzogranite are higher than those of the Dağbaşı (0.51237–0.51260), Camiboğazı (0.51240–0.51252), Turnagöl (0.51238–0.51240), and Jindong (0.51254–0.51263) plutons.

All data and observations provide a genetic model that includes melt-interactions of dehydration melting of mafic meta-igneous (meta-basalt or amphibolite) lower crustal. Most major oxide and trace element variations of Eğrikar Monzogranite show positive or negative correlations with increasing SiO_2 contents (Figure 7), thereby playing the significant role of the FC processes of the different mineral phases during the evolution of Eğrikar Monzogranite. The rocks are characterized by low CaO and Sr contents and have small negative Ba, Sr, and Eu anomalies (Figures 7–9). Eğrikar Monzogranite has strongly negative Eu anomalies

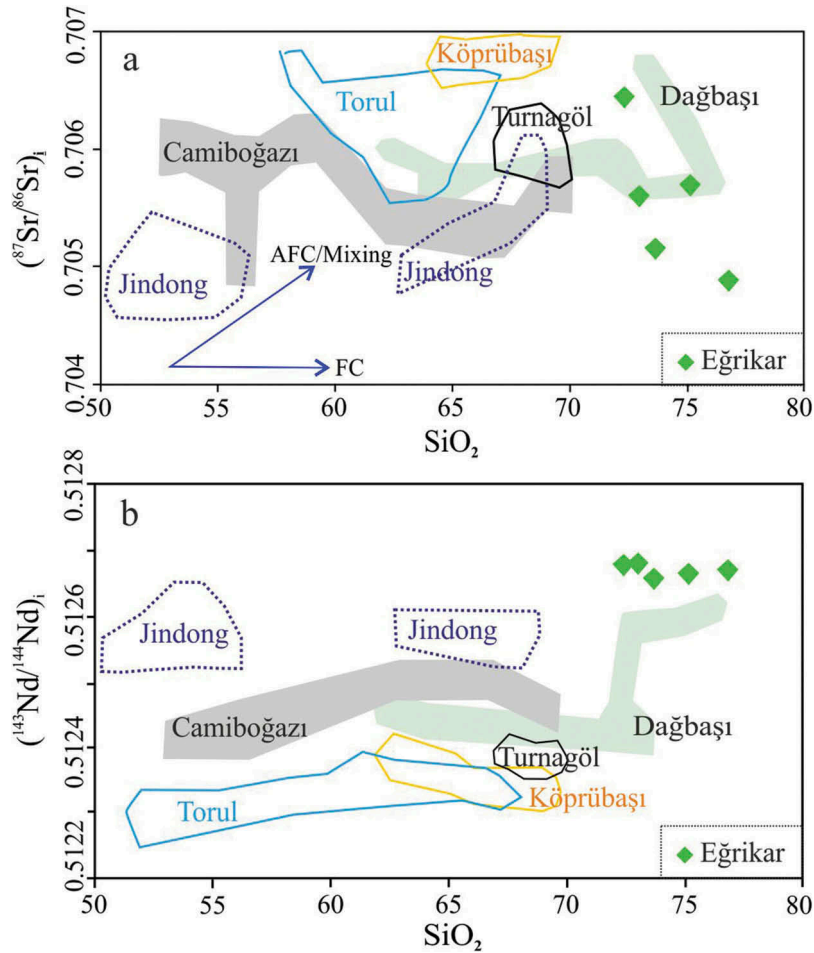


Figure 10. In Eğrikar Monzogranite, (a) SiO₂ vs. ⁸⁷Sr/⁸⁶Sr_(i) and b) SiO₂ vs. ¹⁴³Nd/¹⁴⁴Nd_(i) diagrams. Dağbaşı Pluton from Kaygusuz and Aydınçakır (2011), Harşit Pluton from Karlı *et al.* (2010), Torul Pluton from Kaygusuz *et al.* (2010), Köprübaşı Pluton from Kaygusuz *et al.* (2012b), Turnagöl Pluton from Kaygusuz *et al.* (2013), Camiboğazı Pluton from Kaygusuz *et al.* (2014), Jindong Plutons from Oh *et al.* (2016).

(mean EuN/Eu* = 0.29–0.65) that are probably associated with plagioclase fractionation (Figure 8). The Al₂O₃, MgO, CaO, Fe₂O_{3T}, and La contents decrease and the K₂O and Ba increase with increasing SiO₂, thereby suggesting biotite, amphibole, and plagioclase FC and accumulations of K-feldspar and sodic plagioclase (Figure 7). Decreases in TiO₂ and P₂O₅ with increasing SiO₂ content may reflect titanite and apatite FC, respectively. The depletion in Zr and Y can report to FC of the accessory phases, such as zircon and titanite. The rocks of Eğrikar Monzogranite are also characterized by negative Nb anomaly (Figure 8), thereby implying a subduction signature or a few crustal contributions. The negative anomalies of Nb, P, and Ti are characteristic features of subduction-related magmas. The negative anomalies of Nb, P, and Ti originated from the relative enrichment of the mantle source via LILE addition from the subducting slab to the mantle, although they may be related to crustal contamination (Borg *et al.* 1997). Crustal components are also rich in

Th 3.5 ppm in the bulk continental crust (Taylor and McLennan 1985). The low Th value (i.e. 3.6–15.2 ppm) in the Eğrikar Monzogranite samples may indicate the lack of effects of crustal contamination. The negative correlation between SiO₂ and ⁸⁷Sr/⁸⁶Sr_(i) and the weak correlation between SiO₂ and ¹⁴³Nd/¹⁴⁴Nd_(i) (Figure 10(a,b)) indicates that assimilation did not play a role in the generation of the monzogranite.

5.3. Source rock

The Y/Nb ratio of granitoids can distinguish between the mantle (Y/Nb < 1.2) and crustal (Y/Nb > 1.2) origins (Eby 1992). The Eğrikar Monzogranite samples have a 1.8:8.1 Y/Nb ratio, thereby suggesting a possible crustal origin for the magma source. The ²⁰⁶Pb/²⁰⁴Pb(i), ²⁰⁷Pb/²⁰⁴Pb(i), and ²⁰⁸Pb/²⁰⁴Pb values (Figure 12) of the Eğrikar Monzogranite samples are obtained in the field of the continental crust (Kempton *et al.* 1997) and are close to the data points from the Torul, Turnagöl,

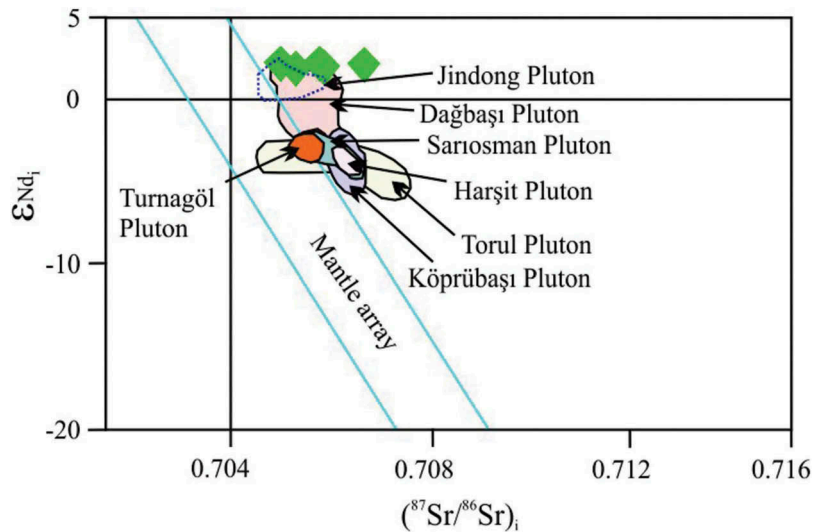


Figure 11. The $^{87}\text{Sr}/^{86}\text{Sr}_t$ vs. $\epsilon_{\text{Nd}(t)}$ diagram of the Eğrikar Monzogranite. Dağbaşı Pluton from Kaygusuz and Aydınçakır (2011), Sarıosman Pluton from Kaygusuz *et al.* (2009), Harşit Pluton from Karlı *et al.* (2010), Torul Pluton from Kaygusuz *et al.* (2010), Köprübaşı Pluton from Kaygusuz *et al.* (2012b), Turnagöl Pluton from Kaygusuz *et al.* (2013), Jindong Pluton from Oh *et al.* (2016).

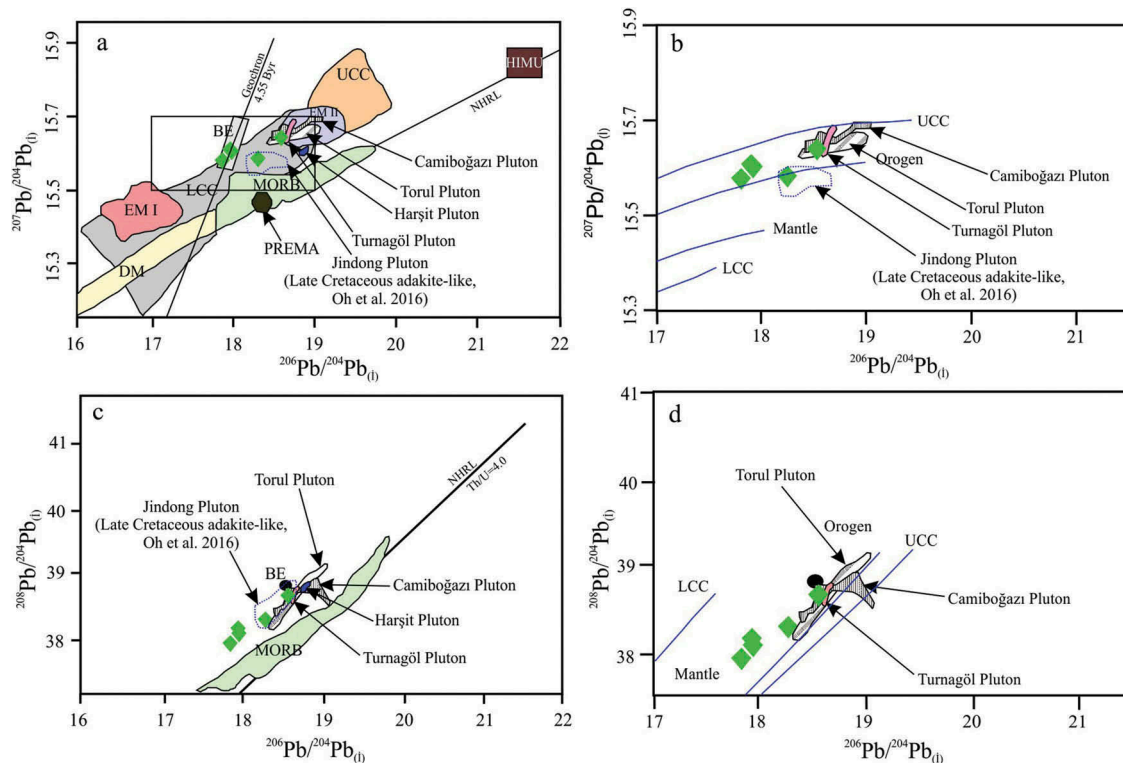


Figure 12. (a) and (b) Plot of $^{206}\text{Pb}/^{204}\text{Pb}_t$ vs. $^{207}\text{Pb}/^{204}\text{Pb}_t$ ratios. (c) and (d) Plot of $^{206}\text{Pb}/^{204}\text{Pb}_t$ vs. $^{208}\text{Pb}/^{204}\text{Pb}_t$ ratios of the Eğrikar Monzogranite. LCC: lower continental crust (Kempton *et al.* 1997), UCC: upper continental crust (Mason *et al.* 1996), MORB: middle ocean rift basalt (Rollinson 1993), EM I and EMII: enrichment mantle (Zindler and Hart 1986), NHRL: Northern Hemisphere reference line (Hart 1984), BE: Bulk earth, HIMU: high μ mantle (Zindler and Hart 1986), DM: depleted mantle (Zindler and Hart 1986), PREMA: prevalent mantle (Zindler and Hart 1986). Harşit Pluton from Karlı *et al.* (2010), Torul Pluton from Kaygusuz *et al.* (2010), Turnagöl Pluton from Kaygusuz *et al.* (2013), Camiboğazi Pluton from Kaygusuz *et al.* (2014), Jindong Pluton from Oh *et al.* (2016).

and Camiboğazi plutons (Kaygusuz *et al.* 2008, 2013, 2014) and Jindong Pluton (Oh *et al.* 2016).

The Eğrikar Monzogranite samples are characterized by high SiO_2 (72–78 wt%) and low Mg# (19–45, except

for one sample), which is consistent with magmas derived from crustal rocks. The Eğrikar Monzogranite samples have low $(\text{Na}_2\text{O}+\text{K}_2\text{O})/(\text{Fe}_2\text{O}_{3\text{T}}+\text{MgO}+\text{TiO}_2)$ and medium $(\text{Na}_2\text{O}+\text{K}_2\text{O}+\text{Fe}_2\text{O}_{3\text{T}}+\text{MgO}+\text{TiO}_2)$ values,

as well as plot in the field of the amphibolite-derived melts (Figure 14(a,b)). The Th/U values of Eğrikar Monzogranite range from 3.27 to 5.63, falling in the field between the continental crustal-derived and N-MORB-derived magmas, similar to the Dağbaşı and Jindong plutons (Figure 13(c)). Furthermore, the Nb–Y–Gax3 ternary plot (Eby 1992) proposes that the magma of the studied monzogranite was generated as a crustal origin resulting from the mantle–crust interactions (Figure 13(d)). The Sr–Nd–Pb isotopic signatures and trace element characteristics of the Campanian Eğrikar Monzogranite have suggested an origin involving amphibolitic lower crustal rocks (Figure 14).

6. Conclusions

Eğrikar Monzogranite is the result of a Late Cretaceous arc-related magmatic activity in the eastern Black Sea region.

Results of the LA–ICP–MS U–Pb zircon dating indicated that the emplacement age of Eğrikar Monzogranite is 78 ± 1.5 Ma. This monzogranite has peraluminous and medium K calc-alkaline characteristics, as well as enriched in LILE and limited in HFSE, thereby showing features of arc-related intrusive rocks. The Eğrikar Monzogranite samples show concave-upward chondrite-normalized REE patterns with negative Eu anomalies. The Eğrikar Monzogranite shows a small range of Sr–Nd–Pb values. It has formed through fractionation of plagioclase, hornblende, biotite, apatite, and zircon; the geochemical and isotopic data indicate that it is generated by partial melting of the mafic lower crustal sources.

Acknowledgements

This research was supported by the 114Y013 numbered The Scientific and Technological Research Council of Turkey

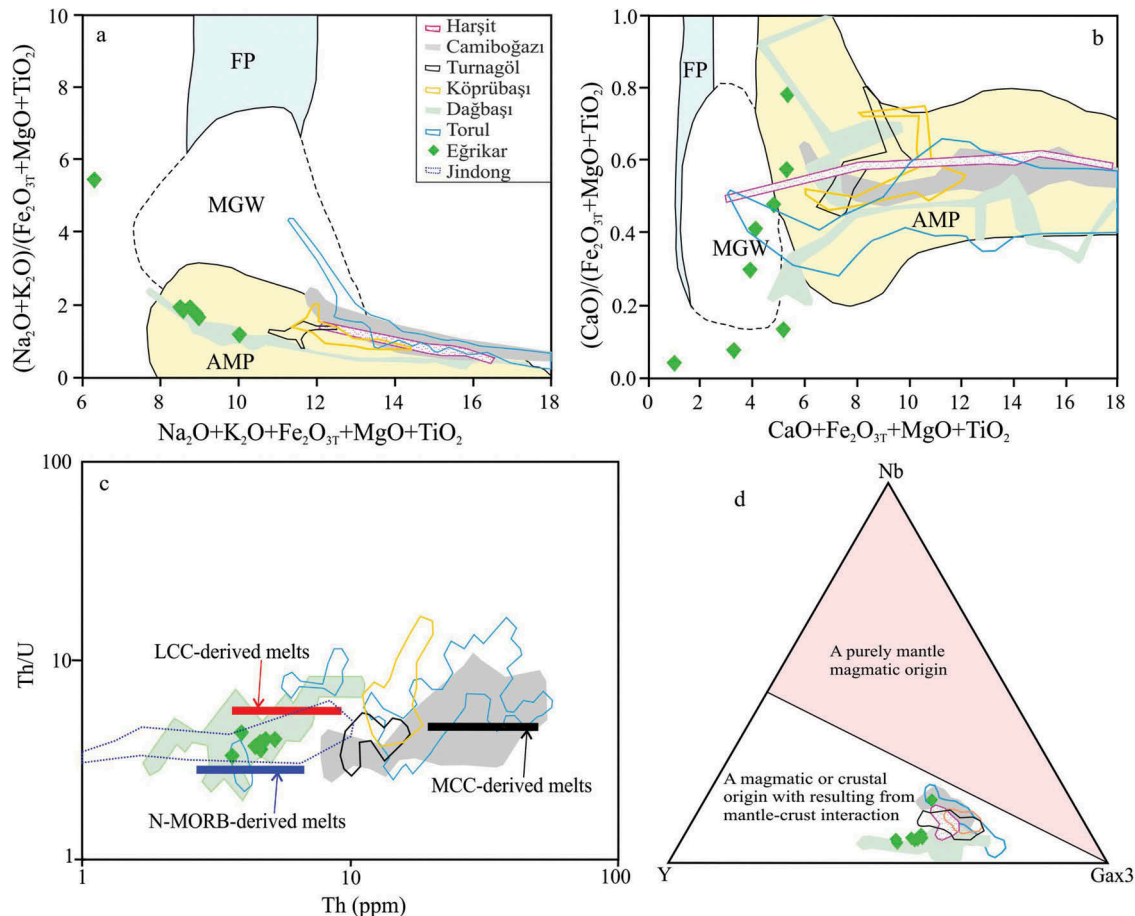


Figure 13. (a) $(\text{Na}_2\text{O}+\text{K}_2\text{O})/(\text{Fe}_2\text{O}_{3\text{T}}+\text{MgO}+\text{TiO}_2)$ vs $(\text{Na}_2\text{O}+\text{K}_2\text{O}+\text{Fe}_2\text{O}_{3\text{T}}+\text{MgO}+\text{TiO}_2)$, (b) $\text{CaO}/(\text{Fe}_2\text{O}_{3\text{T}}+\text{MgO}+\text{TiO}_2)$ vs $(\text{CaO}+\text{Fe}_2\text{O}_{3\text{T}}+\text{MgO}+\text{TiO}_2)$, (c) Th/U vs. Th and (d) Nb–Y–Gax3 ternary (Eby 1992) diagrams for samples from the Eğrikar Monzogranite. FP: felsic pelites, MGW: metagraywacke; MP: metapelite; AMP: amphibolite. Data source: Patiño Douce (1999). LCC: lower continental crust, MCC: middle continental crust. The compositions of lower and middle continental crusts were taken from Rudnick and Gao (2003). N-MORB is from Sun *et al.* (2008). Dağbaşı Pluton from Kaygusuz and Aydınçakır (2011), Harşit Pluton from Karslı *et al.* (2010), Torul Pluton from Kaygusuz *et al.* (2010), Köprübaşı Pluton from Kaygusuz *et al.* (2012b), Turnagöl Pluton from Kaygusuz *et al.* (2013), Camiboğazı Pluton *et al.* (2014).

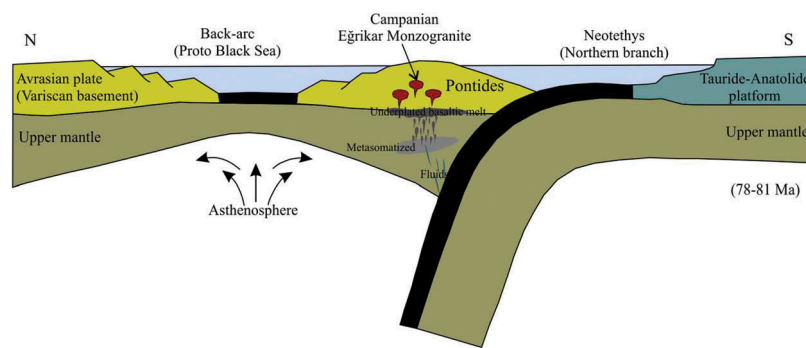


Figure 14. Schematic model for the magma evolution and emplacement of Campanian Eğrikar Monzogranite from eastern Pontides in NE Turkey modified from Karslı *et al.* (2010).

(TÜBİTAK). Authors thank Dr Robert J. Stern, editor-in-Chief, who provided many comments that improved the content of the manuscript, and anonymous reviewers for their constructive criticisms. Meltem Yılmaz, Enes Türk, and Tanju Aydurmuş are thanked for their help during the fieldwork.

Disclosure statement

No potential conflict of interest was reported by the authors.

Funding

This research was supported by the 114Y013 numbered The Scientific and Technological Research Council of Turkey (TÜBİTAK).

References

- Akaryalı, E., 2016, Geochemical, fluid inclusion and isotopic (O, H and S) constraints on the origin of Pb–Zn±Au vein-type mineralizations in the Eastern Pontides Orogenic Belt (NE Turkey): *Ore Geology Reviews*, v. 74, p. 1–14. doi:10.1016/j.oregeorev.2015.11.013
- Akaryalı, E., and Akbulut, K., 2016, Constraints of C–O–S isotope compositions and the origin of the Ünlüpinar volcanic-hosted epithermal Pb–Zn±Au deposit, Gümüşhane, NE Turkey: *Journal of Asian Earth Sciences*, v. 117, p. 119–134. doi:10.1016/j.jseaes.2015.12.012
- Altherr, R., and Siebel, W., 2002, I-type plutonism in a continental back-arc setting: Miocene granitoids and monzonites from the central Aegean Sea, Greece: *Contributions to Mineralogy and Petrology*, v. 143, p. 397–415. doi:10.1007/s00410-002-0352-y
- Andersen, T., 2002, Correction of common lead in U–Pb analyses that do not report ²⁰⁴Pb: *Chemical Geology*, v. 192, p. 59–79. doi:10.1016/S0009-2541(02)00195-X
- Arslan, M., and Aslan, Z., 2006, Mineralogy, petrography and whole-rock geochemistry of the Tertiary granitic intrusions in the Eastern Pontides, Turkey: *Journal of Asian Earth Sciences*, v. 27, p. 177–193. doi:10.1016/j.jseaes.2005.03.002
- Arslan, M., Tüysüz, N., Korkmaz, S., and Kurt, H., 1997, Geochemistry and petrogenesis of the Eastern Pontide Volcanic Rocks, Northeast Turkey: *Chemie der Erde*, v. 57, p. 157–187.
- Aydınçakır, E., 2014, The petrogenesis of Early Eocene non-adakitic volcanism in NE Turkey: Constraints on the geodynamic implications: *Lithos*, v. 208–209, p. 361–377. doi:10.1016/j.lithos.2014.08.019
- Aydınçakır, E., and Şen, C., 2014, Petrogenesis of the post-collisional volcanic rocks from the Borçka (Artvin) area: Implications for the evolution of the Eocene magmatism in the Eastern Pontides (NE Turkey): *Lithos*, v. 172–173, p. 98–117.
- Bacon, C.R., and Dritsch, T.H., 1988, Compositional evolution of the zoned calc-alkaline magma chamber of Mount Mazama, Crater Lake, Oregon: *Contributions to Mineralogy and Petrology*, v. 98, p. 224–256. doi:10.1007/BF00402114
- Black, L.P., Kamo, S.L., Allen, C.M., Aleinikoff, J.N., Davis, D.W., Korsch, R.J., and Foudoulis, C., 2003, TEMORA 1: A new zircon standard for Phanerozoic U–Pb geochronology: *Chemical Geology*, v. 200, p. 155–170. doi:10.1016/S0009-2541(03)00165-7
- Borg, L.E., Nyquist, L.E., Wiesmann, H., and Shih, C.Y., 1997, Constraints on Martian differentiation processes from Rb–Sr and Sm–Nd isotopic analyses of the basaltic shergottite QUE94201: *Geochimica Et Cosmochimica Acta*, v. 61, p. 4915–4931. doi:10.1016/S0016-7037(97)00276-7
- Boynton, W.V., 1984, Cosmochemistry of the rare earth elements; *Meteorite Studies*, in Henderson, P., Editor, Rare earth element geochemistry: Amsterdam, Elsevier Sci. Publ. Co., p. 63–114.
- Boztuğ, D., Erçin, A.I., Kuruçelik, M.K., Goç, D., Kömür, I., and Iskenderoglu, A., 2006, Geochemical characteristics of the composite Kaçkar batholith generated in a Neo-Tethyan convergence system, Eastern Pontides, Turkey: *Journal of Asian Earth Sciences*, v. 27, p. 286–302. doi:10.1016/j.jseaes.2005.03.008
- Boztuğ, D., Jonckheere, R., Wagner, G.A., and Yegingil, Z., 2004, Slow Senonian and fast Palaeocene–Early Eocene uplift of the granitoids in the Central Eastern Pontides, Turkey: Apatite fission-track results: *Tectonophysics*, v. 382, p. 213–228. doi:10.1016/j.tecto.2004.01.001
- Boztuğ, D., Kuşçu, I., Erçin, A.I., Avcı, N., and Şahin, S.Y., 2003, Mineral deposits associated with the pre-, syn- and post-collisional granitoids of the neo-Tethyan convergence system between the Eurasian and Anatolian plates in NE and

- Central Turkey, in Eliopoulou, D., et al., eds, *Mineral exploration and sustainable development*: Rotterdam, Millpress, p. 1141–1144.
- Çamur, M.Z., Güven, I.H., and Er, M., 1996, Geochemical characteristics of the Eastern Pontide volcanics: An example of multiple volcanic cycles in arc evolution: *Turkish Journal of Earth Sciences*, v. 5, p. 123–144.
- Chappell, B.W., and White, A.J.R., 1992, I- and S-type granites in the Lachlan Fold Belt: Transition of the Royal Society Edinburgh *Earth Science*, v. 83, p. 1–26. doi:10.1017/S0263593300007720
- Chen, B., Jahn, B.M., and Wei, C., 2002, Petrogenesis of Mesozoic granitoids in the Dabie UHP complex, Central China: Trace element and Nd–Sr isotope evidence: *Lithos*, v. 60, p. 67–88. doi:10.1016/S0024-4937(01)00077-9
- Delibaş, O., Moritz, R., Ulianov, A., Chiaradia, M., Revan, K.M., Göç, D., and Saraç, C., 2016, Cretaceous subduction-related magmatism and associated porphyry-type Cu–Mo prospects in the Eastern Pontides, Turkey: New constraints from geochronology and geochemistry: *Lithos*, v. 248–251, p. 119–137. doi:10.1016/j.lithos.2016.01.020
- Dokuz, A., 2011, A slab detachment and delamination model for the generation of Carboniferous high-potassium I-type magmatism in the eastern Pontides, NE Turkey: The Köse composite pluton: *Gondwana Research*, v. 19, p. 926–944. doi:10.1016/j.gr.2010.09.006
- Dokuz, A., Karsli, O., Chen, B., and Uysal, İ., 2010, Sources and petrogenesis of Jurassic granitoids in the Yusufeli area, Northeastern Turkey: Implications for pre- and postcollisional lithospheric thinning of the Eastern Pontides: *Tectonophysics*, v. 480, p. 259–279. doi:10.1016/j.tecto.2009.10.009
- Eby, G.N., 1992, Chemical subdivision of the A-type granitoids: Petrogenetic and tectonic implications: *Geology*, v. 20, p. 641–644. doi:10.1130/0091-7613(1992)020<0641:CSOTAT>2.3.CO;2
- Eyüboğlu, Y., Chung, S.L., Santosh, M., Dudas, F.O., and Akaryali, E., 2011a, Transition from shoshonitic to adakitic magmatism in the Eastern Pontides, NE Turkey: Implications for slab window melting: *Gondwana Research*, v. 19, p. 413–429. doi:10.1016/j.gr.2010.07.006
- Eyüboğlu, Y., Dudas, F.O., Santosh, M., Zhu, D.C., Yi, K., Chatterjee, N., Jeong, Y.J., Akaryali, E., and Liu, Z., 2015, Cenozoic forearc gabbros from the northern zone of the Eastern Pontides Orogenic Belt, NE Turkey: Implications for slab window magmatism and convergent margin tectonics: *Gondwana Research*, v. 33, p. 160–189. doi:10.1016/j.gr.2015.07.006
- Eyüboğlu, Y., Santosh, M., and Chung, S.L., 2011, Petrochemistry and U–Pb zircon ages of adakitic intrusions from the Pular Massif (Eastern Pontides, NE Turkey): Implications for slab rollback and ridge subduction associated with Cenozoic convergent tectonics in Eastern Mediterranean: *Journal of Geology*, v. 119, p. 394–417. doi:10.1086/660158
- Faure, G., and Mensing, T.M., 2005, *Isotopes: Principles and applications* (3rd edition): NJ, USA, John Wiley and Sons, 897 p.
- Gedik, A., Ercan, T., Korkmaz, S., and Karataş, S., 1992, Rize-Fındıklı-Çamlıhemşin arasında (Doğu Karadeniz) yer alan mağmatik kayaların petrolojisi ve Doğu Pontidlerdeki bölgesel yayılımları: *Geological Bulletin of Turkey*, v. 35, p. 15–38.
- Gedikoğlu, A., 1978, Harşit Granit Karmaşığı ve Çevre Kayaçları [Doçentlik Tezi]: Trabzon, K.T.Ü. Yer Bilimleri Fakültesi
- Grove, T.L., and Donnelly-Nolan, J.M., 1986, The evolution of young silicic lavas at Medicine Lake Volcano, California: Implications for the origin of compositional gaps in calcalkaline series lavas: *Contributions to Mineralogy and Petrology*, v. 92, p. 281–302. doi:10.1007/BF00572157
- Hanchar, J.M., and Watson, E.B., 2003, Zircon saturation thermometry, in Hanchar, J.M., and Hoskin, P.W.O., eds., *Zircon, review in mineralogy and geochemistry*, Vol. 53: Mineralogical Society of America, Geochemical Society of America, p. 89–112.
- Harris, N.B.W., Pearce, J.A., and Tindle, A.G., 1986, *Geochemical characteristics of collision-zone magmatism*, v. 19: London, Geological Society, Special Publication, p. 67–81.
- Hart, S.R., 1984, A large scale isotope anomaly in the Southern Hemisphere mantle: *Science*, v. 309, p. 753–757.
- Hastie, A.R., Kerr, A.C., Pearce, J.A., and Mitchell, S.F., 2007, Classification of altered volcanic island arc rocks using immobile trace elements: Development of the Th–Co discrimination diagram: *Journal of Petrology*, v. 48, p. 2341–2357. doi:10.1093/petrology/egm062
- Irvine, L.C., and Baragar, W.R.A., 1971, A guide to chemical classification of the common volcanic rocks: *Canadian Journal of Earth Sciences*, v. 8, p. 523–548. doi:10.1139/e71-055
- Jacobsen, S.B., and Wasserburg, G.J., 1980, Sm–Nd isotopic evolution of chondrites: *Earth and Planetary Science Letters*, v. 50, p. 139–155. doi:10.1016/0012-821X(80)90125-9
- Jica, 1986, The republic of Turkey report on the cooperative mineral exploration of Gümüşhane area, consolidated report: Japanese Int. Coop. Agency, Ankara, Turkey (Unpublished), 146 p.
- Karsli, O., Dokuz, A., Uysal, İ., Aydın, F., Chen, B., Kandemir, R., and Wijbrans, J., 2010, Relative contributions of crust and mantle to generation of Campanian high-K calcalkaline I-type granitoids in a subduction setting, with special reference to the Harşit Pluton, Eastern Turkey: *Contributions to Mineralogy and Petrology*, v. 160, p. 467–487. doi:10.1007/s00410-010-0489-z
- Kaygusuz, A., Arslan, M., İlbeyli, N., and Sipahi, F., 2012b, Doğu Pontid kuzey zonu ve kuzey-güney zon geçişinde yüzeylenen Kretase-Paleosen yaşlı granitoidik sokulumların petrokimyası, Sr–Nd–Pb–O izotop jeokimyası, jeokronolojisi ve jeodinamik gelişimi, Tübitak Çaydağ Project No: 109Y052 final report (Turkish with English Abstract), 175 p.
- Kaygusuz, A., Arslan, M., Siebel, W., Sipahi, F., and İlbeyli, N., 2012a, Geochronological evidence and tectonic significance of Carboniferous magmatism in the southwest Trabzon area, eastern Pontides, Turkey: *International Geology Review*, v. 54, no. 15, p. 1776–1800. doi:10.1080/00206814.2012.676371
- Kaygusuz, A., Arslan, M., Siebel, W., Sipahi, F., İlbeyli, N., and Temizel, İ., 2014, LA-ICP MS zircon dating, whole-rock and Sr–Nd–Pb–O isotope geochemistry of the Camiboğazi pluton, Eastern Pontides, NE Turkey: Implications for lithospheric mantle and lower crustal sources in arc-related

- I-type magmatism: *Lithos*, v. 192-195, p. 271–290. doi:10.1016/j.lithos.2014.02.014
- Kaygusuz, A., Arslan, M., Sipahi, F., and Temizel, İ., 2016, U-Pb zircon chronology and petrogenesis of carboniferous plutons in the northern part of the Eastern Pontides, NE Turkey: Constraints for Paleozoic magmatism and geodynamic evolution: *Gondwana Research*, v. 39, p. 327–346. doi:10.1016/j.gr.2016.01.011
- Kaygusuz, A., and Aydınçakır, E., 2011, Petrogenesis of a late cretaceous composite pluton from the eastern Pontides: The Dağbaşı pluton, NE Turkey: *Neues Jahrbuch Für Mineralogie Abhandlungen*, v. 188, p. 211–233. doi:10.1127/0077-7757/2011/0201
- Kaygusuz, A., Chen, B., Aslan, Z., Siebel, W., and Şen, C., 2009, U-Pb zircon SHRIMP ages, geochemical and Sr-Nd isotopic compositions of the early Cretaceous I-type Sariosman pluton, Eastern Pontides, NE Turkey: *Turkish Journal of Earth Science*, v. 18, p. 549–581.
- Kaygusuz, A., and Şen, C., 2011, Calc-alkaline I-type plutons in the eastern Pontides, NE Turkey: U-Pb zircon ages, geochemical and Sr-Nd isotopic compositions: *Chemie der Erde-Geochemistry*, v. 71, p. 59–75. doi:10.1016/j.chemer.2010.07.005
- Kaygusuz, A., Siebel, W., İlbeyli, N., Arslan, M., Satır, M., and Şen, C., 2010, Insight into magma genesis at convergent plate margins – a case study from the eastern Pontides (NE Turkey): *Neues Jahrbuch Für Mineralogie - Abhandlungen*, v. 187, no. 3, p. 265–287. doi:10.1127/0077-7757/2010/0178
- Kaygusuz, A., Siebel, W., Şen, C., and Satır, M., 2008, Petrochemistry and petrology of I-type granitoids in an arc setting: The composite Torul pluton, Eastern Pontides, NE Turkey: *International Journal Earth Science*, v. 97, p. 739–764. doi:10.1007/s00531-007-0188-9
- Kaygusuz, A., Sipahi, F., İlbeyli, N., Arslan, M., Chen, B., and Aydınçakır, E., 2013, Petrogenesis of the Late Cretaceous Turnagöl intrusion in the eastern Pontides: Implications for magma genesis in the arc setting: *Geoscience Frontiers*, v. 4, p. 423–438. doi:10.1016/j.gsf.2012.09.003
- Kempton, P.D., Downes, H., and Embey-Istzin, A., 1997, Mafic granulite xenoliths in Neogene alkali basalts from the western Pannonian basin: Insights into the lower crust of a collapsed orogen: *Journal of Petrology*, v. 38, p. 941–970. doi:10.1093/ptro/38.7.941
- Kolb, M., Von Quadt, A., Peytcheva, I., Heinrich, C.A., Fowler, S. J., and Cvetkovic, V., 2013, Adakite-like and normal arc magmas: Distinct fractionation paths in the East Serbian segment of the Balkan-Carpathian arc: *Journal of Petrology*, v. 54, p. 421–451. doi:10.1093/ptrology/egs072
- Ludwig, K.R., 2003, User's manual for isoplot 3.0: A geochronological toolkit for microsoft excel: Berkeley Geochronology Center, Special Publication, v. 4, p. 1–71.
- Mason, P.R.D., Downes, H., Thirlwall, M.F., Seghedi, I., Szakács, A., Lowry, D., and Mattery, D., 1996, Crystal assimilation as a major petrogenetic process in the East Carpathian Neogene and Quaternary continental margin arc, Romania: *Journal of Petrology*, v. 37, p. 927–959. doi:10.1093/ptrology/37.4.927
- McCulloch, M.T., and Gamble, J.A., 1991, Geochemical and geodynamical constraints on subduction zone magmatism: *Earth and Planetary Science Letters*, v. 102, p. 358–374. doi:10.1016/0012-821X(91)90029-H
- Middlemost, E.A.K., 1994, Naming materials in the magma/igneous rock system: *Earth Science Review*, v. 37, p. 215–224. doi:10.1016/0012-8252(94)90029-9
- Miller, C.F., Meschter McDowell, S., and Mapes, R.W., 2003, Hot and cold granites? Implications of zircon saturation temperatures and preservation of inheritance: *Geology*, v. 31, p. 529–532. doi:10.1130/0091-7613(2003)031<0529:HACGIO>2.0.CO;2
- Moore, W.J., McKee, E.H., and Akıncı, Ö., 1980, Chemistry and chronology of plutonic rocks in the Pontid mountains, northern Turkey. *in* Symposium of European Copper Deposits, Belgrade, p. 209–216.
- General Directorate of Mineral Research and Exploration (MTA), 2011, Geological map of Turkey: MTA general directorate of mineral research and exploration: Ankara, Turkey.
- Nikishin, A.M., Korotaev, M.V., Ershov, A., and Brunet, M.F., 2003, The Black Sea basin: Tectonic history and Neogene-Quaternary rapid subsidence modeling: *Sedimentary Geology*, v. 156, p. 149–168. doi:10.1016/S0037-0738(02)00286-5
- Oh, J.I., Choi, S.H., and Yi, K., 2016, Origin of adakite-like plutons in southern Korea: *Lithos*, v. 262, p. 620–635. doi:10.1016/j.lithos.2016.07.040
- Okay, A.I., and Şahintürk, Ö., 1997, Geology of the Eastern Pontides, *in* Robinson, A.G., ed., Regional and petroleum geology of the Black Sea and surrounding region, Vol. 68: AAPG Memoir, p. 291–310.
- Okay, A.I., and Tüysüz, O., 1999, Tethyan sutures of northern Turkey, *in* Durand, B., Jolivet, L., Horvath, F., and Seranne, M., eds., The mediterranean basins: Tertiary extension within the Alpine orogen, Vol. 156: Geological Society, Special Publication, p. 475–515.
- Patiño Douce, A.E., 1999, What do experiments tell us about the relative contributions of crust and mantle to the origin of granitic magmas? *in* Castro, A., Fernandez, C., and Vigneresse, J.L., eds., Understanding granites: Integrating new and classical techniques, Vol. 168; London, Geological Society, Special Publications, p. 55–75.
- Pearce, J.A., Harris, N.B.W., and Tindle, A.G., 1984, Trace element discrimination diagram for the tectonic interpretation of granitic rocks: *Journal of Petrology*, v. 25, p. 956–983. doi:10.1093/ptrology/25.4.956
- Pupin, J.P., 1980, Zircon and granite petrology: *Contributions to Mineralogy and Petrology*, v. 73, p. 207–220. doi:10.1007/BF00381441
- Ramos, F.C., 1992, Isotope Geology of Metamorphic Core of the Central Grouse Creek Mountains, Box Elder Country, Utah [MSc thesis]; Los Angeles, University of California.
- Roberts, M.P., and Clemens, J.D., 1993, Origin of high-potassium, calc-alkaline, I-type granitoids: *Geology*, v. 21, p. 825–828. doi:10.1130/0091-7613(1993)021<0825:OOHPTA>2.3.CO;2
- Rolland, Y., Galoyan, G., Sosson, M., Melkonyan, R., and Avagyan, A., 2010, The Armenian Ophiolite: Insights for Jurassic back-arc formation, Lower Cretaceous hot spot magmatism and Upper Cretaceous obduction over the South Armenian Block, *in* Sosson, M., Kaymakci, N., Stephenson, R.A., Bergerat, F., and Starostenko, V., Eds, Sedimentary basin tectonics from the Black Sea and Caucasus to the Arabian Platform, Vol. 340; London, Geological Society, Special Publications, p. 353–382.

- Rollinson, H.R., 1993, Using geochemical data: Evaluation, presentation, interpretation: Essex, Longman Scientific and Technical, p. 350.
- Rudnick, R.L., and Gao, S., 2003, Composition of the continental crust, in Holland, H.D., and Turekian, K.K., eds., Treatise on Geochemistry, Vol. 3: Oxford: Elsevier, p. 1–64.
- Saydam Eker, C., Sipahi, F., and Kaygusuz, A., 2012, Trace and rare earth elements as indicators of provenance and depositional environments of Lias Cherts in Gumushane, NE Turkey: *Chemie der Erde/Geochemistry*, v. 72, no. 2, p. 167–177.
- Şen, C., 2007, Jurassic volcanism in the eastern pontides: Is it rift related or subduction related? *Turkish Journal of Earth Sciences*, v. 16, p. 523–539.
- Şengör, A.M.C., and Yılmaz, Y., 1981, Tethyan evolution of Turkey: A plate tectonic approach: *Tectonophysics*, v. 75, p. 181–241. doi:10.1016/0040-1951(81)90275-4
- Sipahi, F., 2011, Formation of skarns at Gümüşhane (Northeastern Turkey): *Neues Jahrbuch für Mineralogie-Abhandlungen*, v. 188, no. 2, p. 169–190. doi:10.1127/0077-7757/2011/0199
- Sipahi, F., and Sadıklar, M.B., 2011, Zigana (Gümüşhane, KDTürkiye) Volkanitlerinin Alterasyon Mineralojisi ve Kütle Değişimi: *Türkiye Jeoloji Bülteni*, v. 53, no. 2–3, p. 122–155.
- Sipahi, F., and Sadıklar, M.B., 2014, Geochemistry of dacitic volcanics in the eastern pontides (NE Turkey): *Geochemistry International*, v. 4, p. 329–349.
- Sipahi, F., Sadıklar, M.B., and Şen, C., 2014, The geochemical and Sr-Nd isotopic Characteristics of Murgul (Artvin) volcanics in the Eastern Black Sea Region (NE Turkey): *Chemie der Erde/Geochemistry*, v. 74, p. 331–342.
- Streckeisen, A., 1976, To each plutonic rock its proper name: *Earth-Science Reviews*, v. 12, p. 1–33. doi:10.1016/0012-8252(76)90052-0
- Sun, S.S., and McDonough, W.F., 1989, Chemical and isotope systematics of oceanic basalts, in Saunders, A.D., and Nory, M.J., eds, Implication for mantle compositions and processes, magmatism in the ocean basins, Vol. 42: London, Geological Society, Special Publications, p. 313–345.
- Sun, W.D., Hu, Y.H., Kamenetsky, V.S., Eggins, S.M., Chen, M., and Arculus, R.J., 2008, Constancy of Nb/U in the mantle revisited: *Geochimica et Cosmochimica Acta*, v. 72, p. 3542–3549. doi:10.1016/j.gca.2008.04.029
- Taner, M.F., 1977, Etuda géologique et pétrographique de la région de Güneyce-İkizdere, située au sud de Rize (Pontides orientales, Turqui e). PhD Thesis, Université de Geneve [unpublished].
- Taylor, S.R., and McLennan, S.M., 1985, The composition and evolution of the continental crust: Rare earth element evidence from sedimentary rocks, *Phil: Transactions R Social*, v. A301, p. 381–399. doi:10.1098/rsta.1981.0119
- Thompson, A.B., and Connolly, J.A.D., 1995, Melting of the continental crust: Some thermal and petrological constraints on anatexis in continental collision zones and other tectonic settings: *Journal of Geophysical Research*, v. 100, p. 15565–15579. doi:10.1029/95JB00191
- Topuz, G., Altherr, R., Schwarz, W.H., Siebel, W., Satir, M., and Dokuz, A., 2005, Postcollisional Plutonism with Adakite-like Signatures: The Eocene Saraycık granodiorite (Eastern Pontides, Turkey): *Contributions to Mineralogy and Petrology*, v. 150, p. 441–455. doi:10.1007/s00410-005-0022-y
- Topuz, G., Altherr, R., Siebel, W., Schwarz, W.H., Zack, T., Hasözbeğ, A., Barth, M., Satir, M., and Şen, C., 2010, Carboniferous high-potassium I-type granitoid magmatism in the Eastern Pontides: The Gümüşhane Pluton (NE Turkey): *Lithos*, v. 116, p. 92–110. doi:10.1016/j.lithos.2010.01.003
- Watson, E.B., and Harrison, T.M., 1983, Zircon saturation revisited temperature and com-position effects in a variety of crustal magma types: *Earth And Planetary Science Letters*, v. 64, p. 295–304. doi:10.1016/0012-821X(83)90211-X
- Whalen, J.B., Currie, K.L., and Chappell, B.W., 1987, A-type granites: Geochemical characteristics, discrimination and petrogenesis: *Contributions to Mineralogy and Petrology*, v. 95, p. 407–419. doi:10.1007/BF00402202
- Wiedenbeck, M., Alle, P., Corfu, F., Griffin, W.L., Meier, M., Oberli, F., Vonquadt, A., Roddick, J.C., and Spiegel, W., 1995, Three natural zircon standards for U-Th-Pb, Lu-Hf, trace-element and REE analyses: *Geostandard Newsletter*, v. 19, p. 1–23. doi:10.1111/j.1751-908X.1995.tb00147.x
- Yılmaz, A., Adamia, S., Chabukiani, A., Chkhotua, T., Erdogan, K., Tuzcu, S., and Karabiyikoglu, M., 2000, Structural correlation of the southern Transcaucasus (Georgia)-eastern Pontides (Turkey), in Bozkurt, E., Winchester, J.A., and Piper, J.D.A., eds., *Tectonics and magmatism in Turkey and surrounding area*, Vol. 173; London, Geological Society, Special Publications, p. 171–182.
- Yılmaz, C., and Korkmaz, S., 1999, Basin development in the eastern Pontides, Jurassic to Cretaceous, NE Turkey: *Zentralblatt für Geologie und Palaöntologie, Teil I*, v. 10-12, p. 1485–1494.
- Yılmaz, S., and Boztuğ, D., 1996, Space and time relations of three plutonic phases in the eastern Pontides, Turkey: *International Geology Review*, v. 38, p. 935–956. doi:10.1080/00206819709465373
- Yılmaz, Y., Tüysüz, O., Yigitbas, E., Genç, S., C., and Sengör, A. M.C., 1997, Geology and tectonic evolution of the Pontides, regional and petroleum geology of the black sea and surrounding region: *American Association Petroleum Geologists Memoir*, v. 68, p. 183–226.
- Yılmaz-Şahin, S., 2005, Transition from arc- to post-collision extensional setting revealed by K-Ar dating and petrology: An example from the granitoids of the eastern Pontide igneous Terrane, Araklı-Trabzon, NE Turkey: *Geological Journal*, v. 40, p. 425–440. doi:10.1002/gj.1020
- Yücel, C., Arslan, M., Temizel, I., and Abdioğlu, E., 2014, Volcanic facies and mineral chemistry of Tertiary volcanics in the northern part of the Eastern Pontides, northeast Turkey: Implications for pre-eruptive crystallization conditions and magma chamber processes: *Mineralogy and Petrology*, v. 108-3, p. 439–467. doi:10.1007/s00710-013-0306-2
- Zartman, R.E., and Doe, B.R., 1981, Plumbotectonics. The model: *Tectonophysics*, v. 75, p. 135–162. doi:10.1016/0040-1951(81)90213-4
- Zindler, A., and Hart, S.R., 1986, Chemical geodynamics: *Annual Review of Earth and Planetary, Sciences*, v. 14, p. 493–571. doi:10.1146/annurev.earth.14.050186.002425